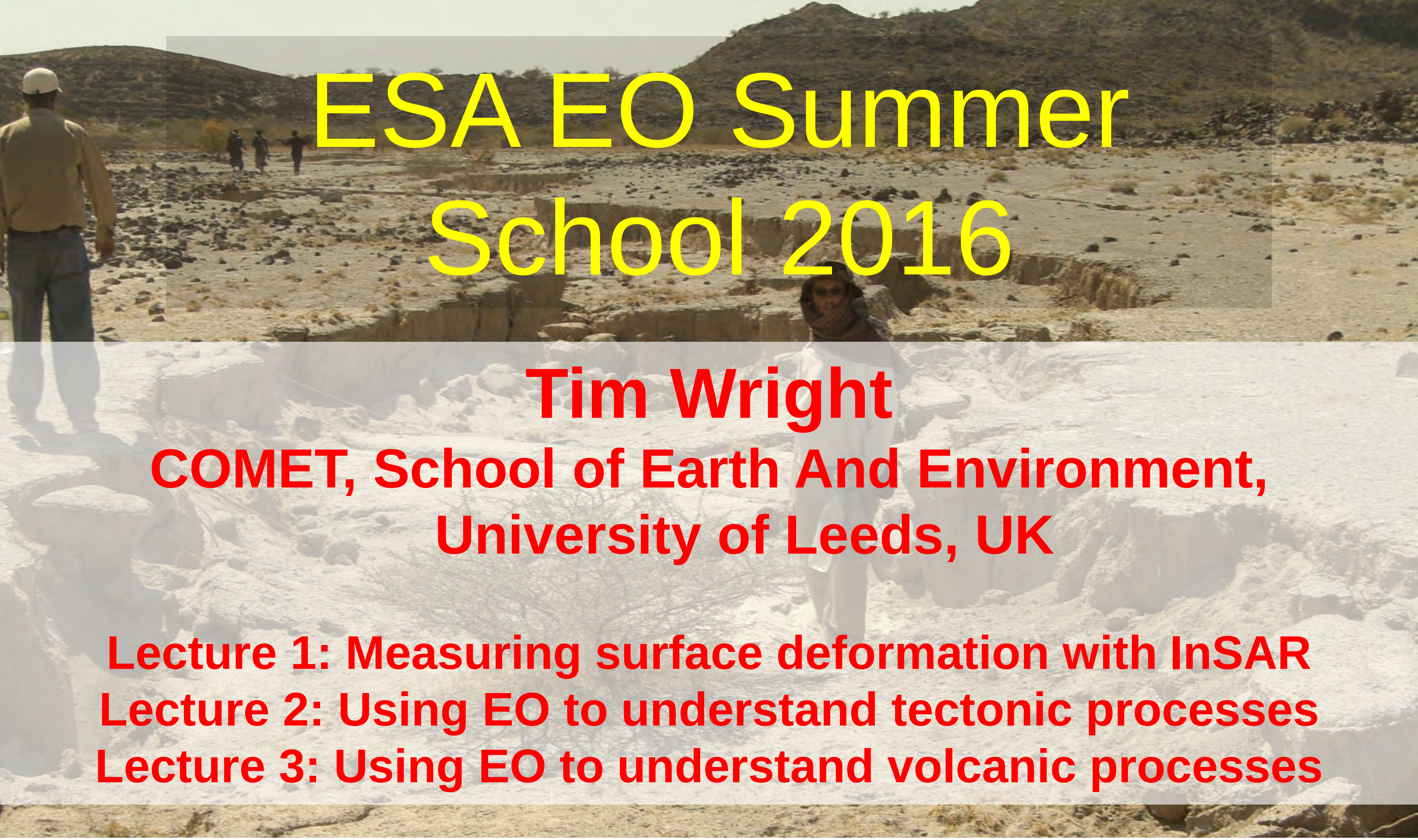

ESA EO Summer School 2016

Tim Wright

COMET, School of Earth And Environment, University of Leeds, UK

Lecture 1: Measuring surface deformation with InSAR
Lecture 2: Using EO to understand tectonic processes
Lecture 3: Using EO to understand volcanic processes

@timwright_leeds
@NERC_COMET

COMET

esa

UNIVERSITY OF LEEDS


Deploying GPS in Afar

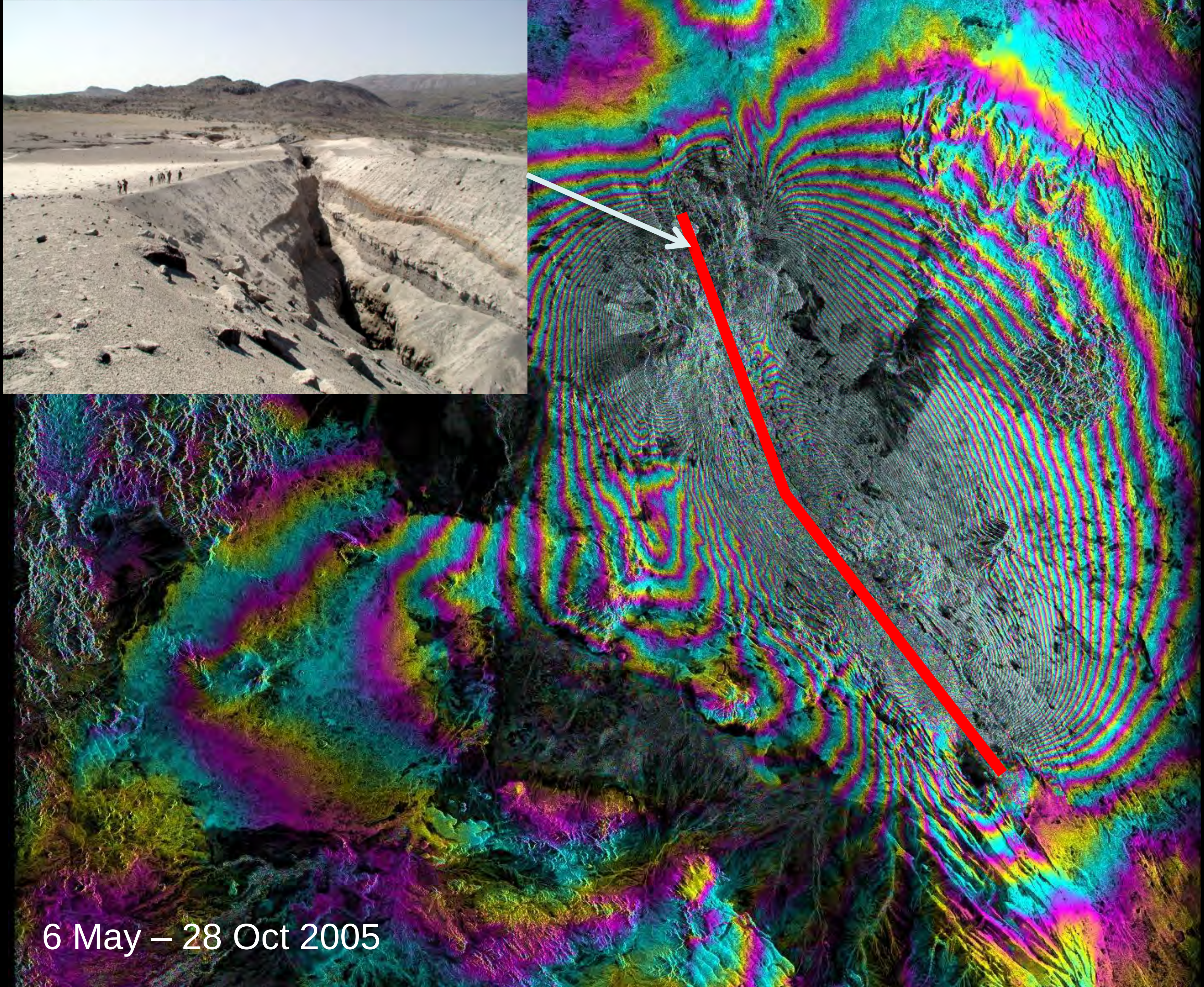
6 May – 28 Oct 2005

Measuring surface deformation with Satellite Radar Interferometry (InSAR)

ESA Summer School, Lecture 1

Outline & Key Points

- Imaging radars – the synthetic aperture
- Satellite radar interferometry
  - How it works
  - Components of interferometric phase
  - Uncertainties associated with InSAR measurements
  - Examples of applications

The Electromagnetic Spectrum

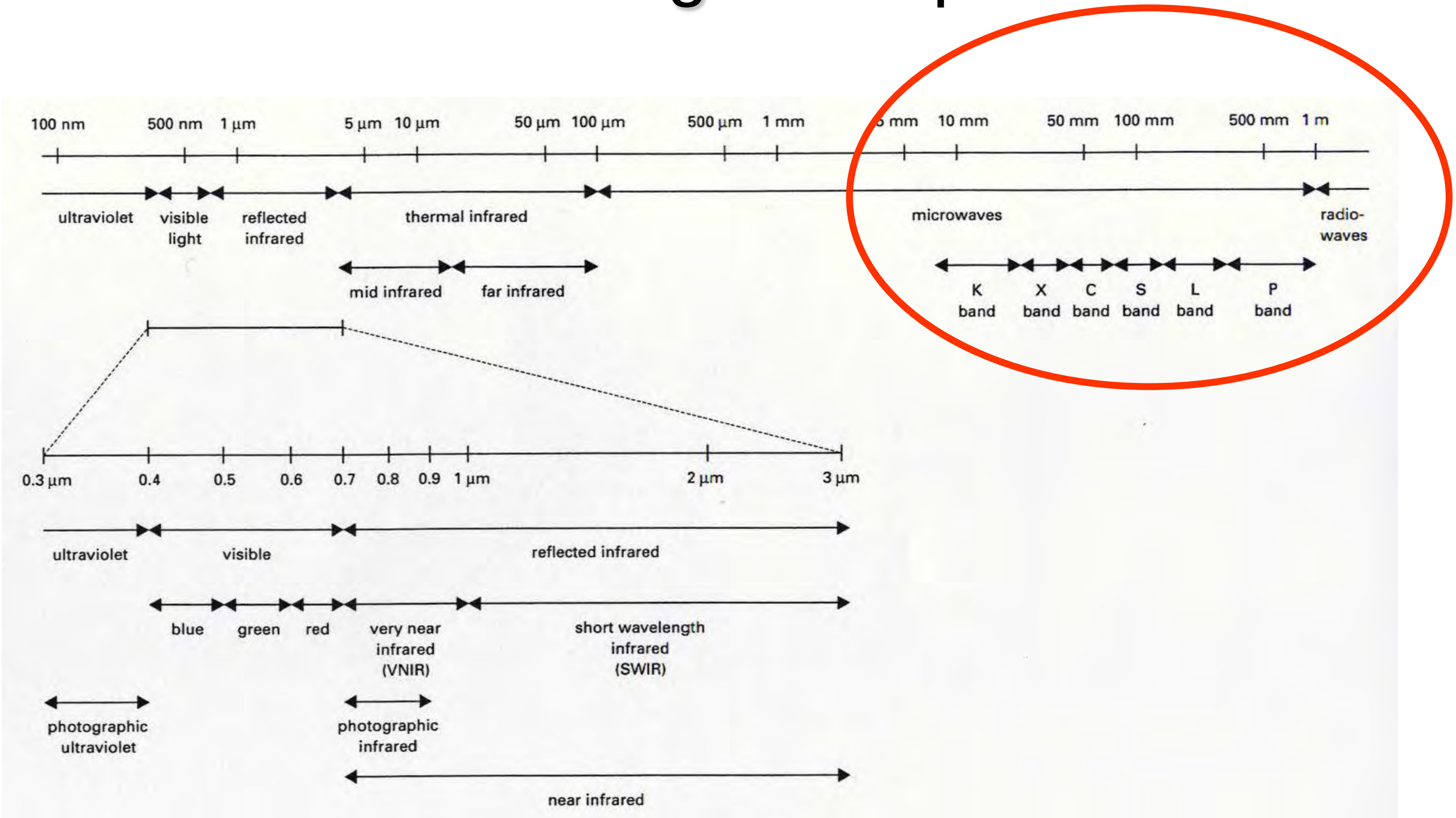

Active Remote Sensing with Microwaves

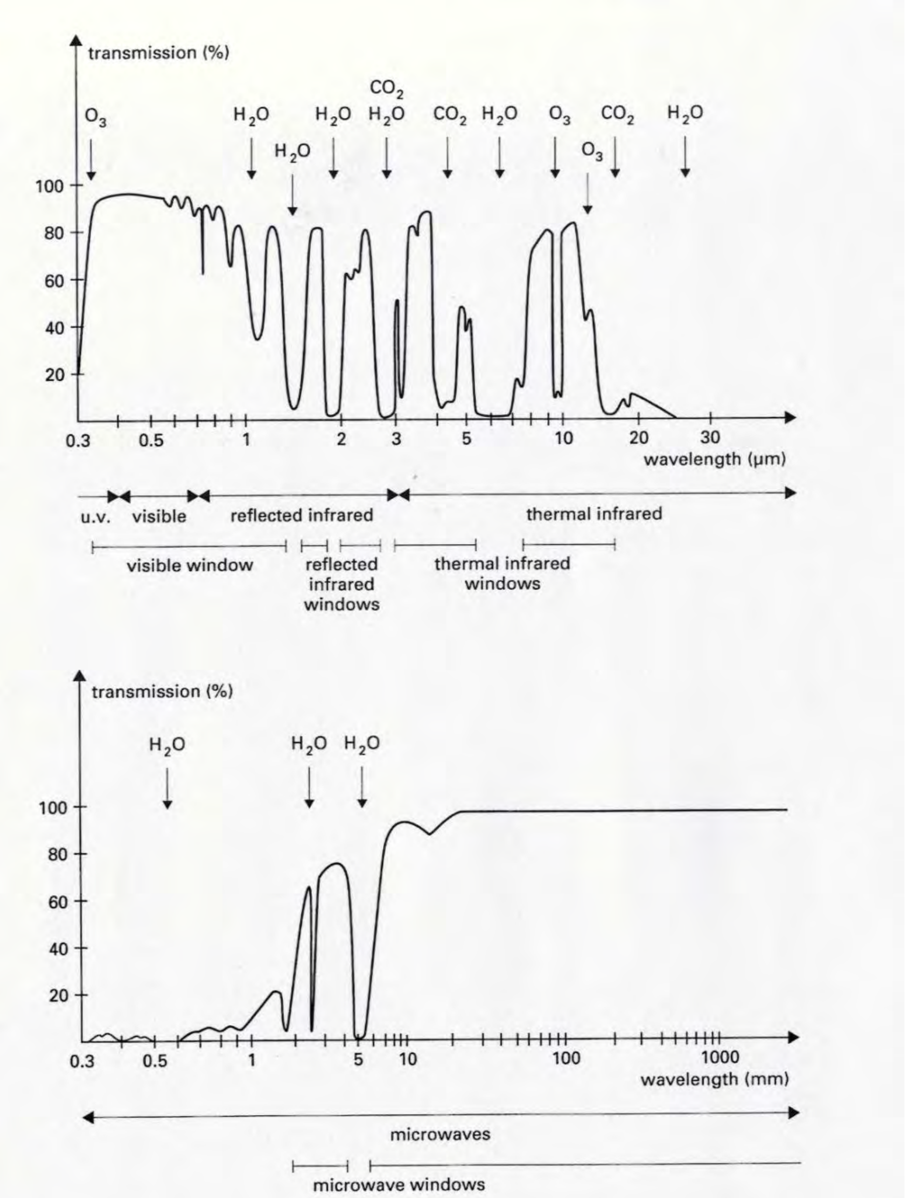

Radar = RAdio Detection And Ranging

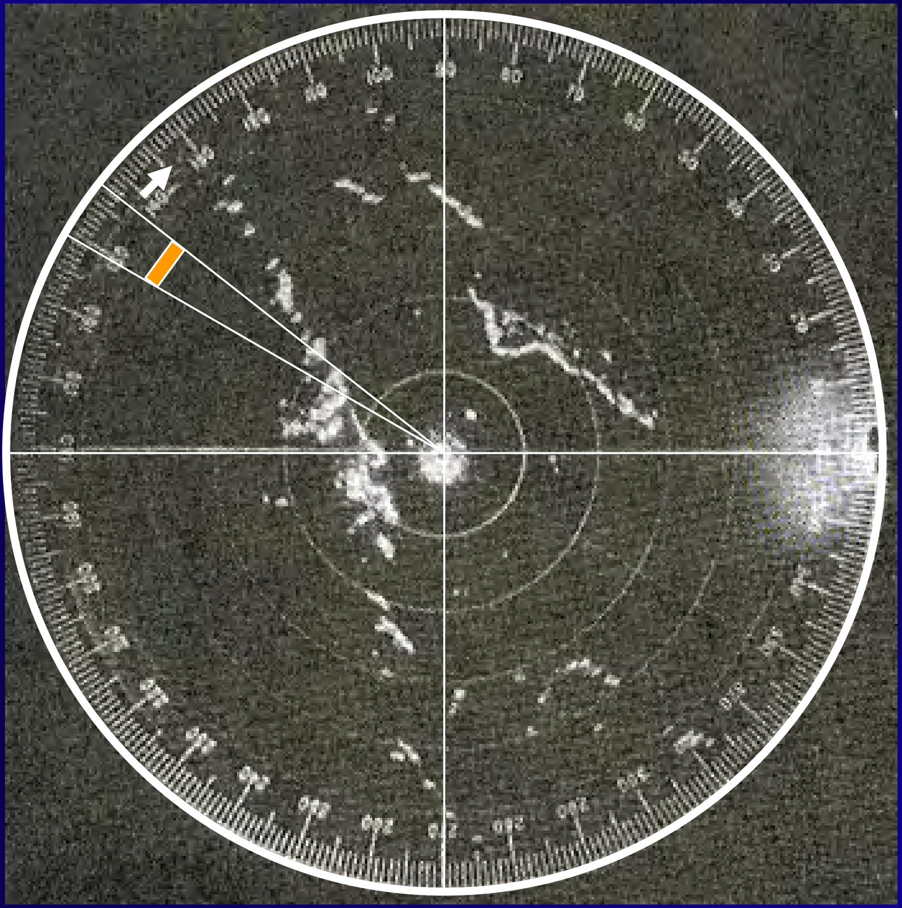

Side-Looking Airborne Radar

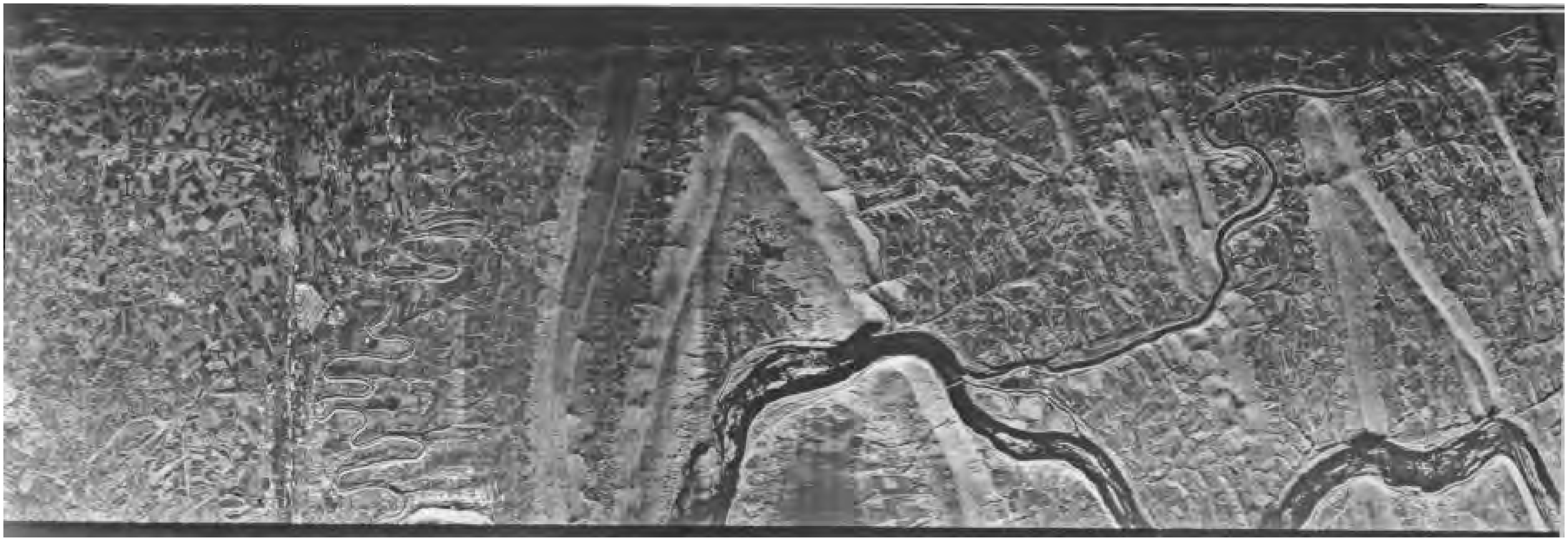

Side-Looking Airborne Radar

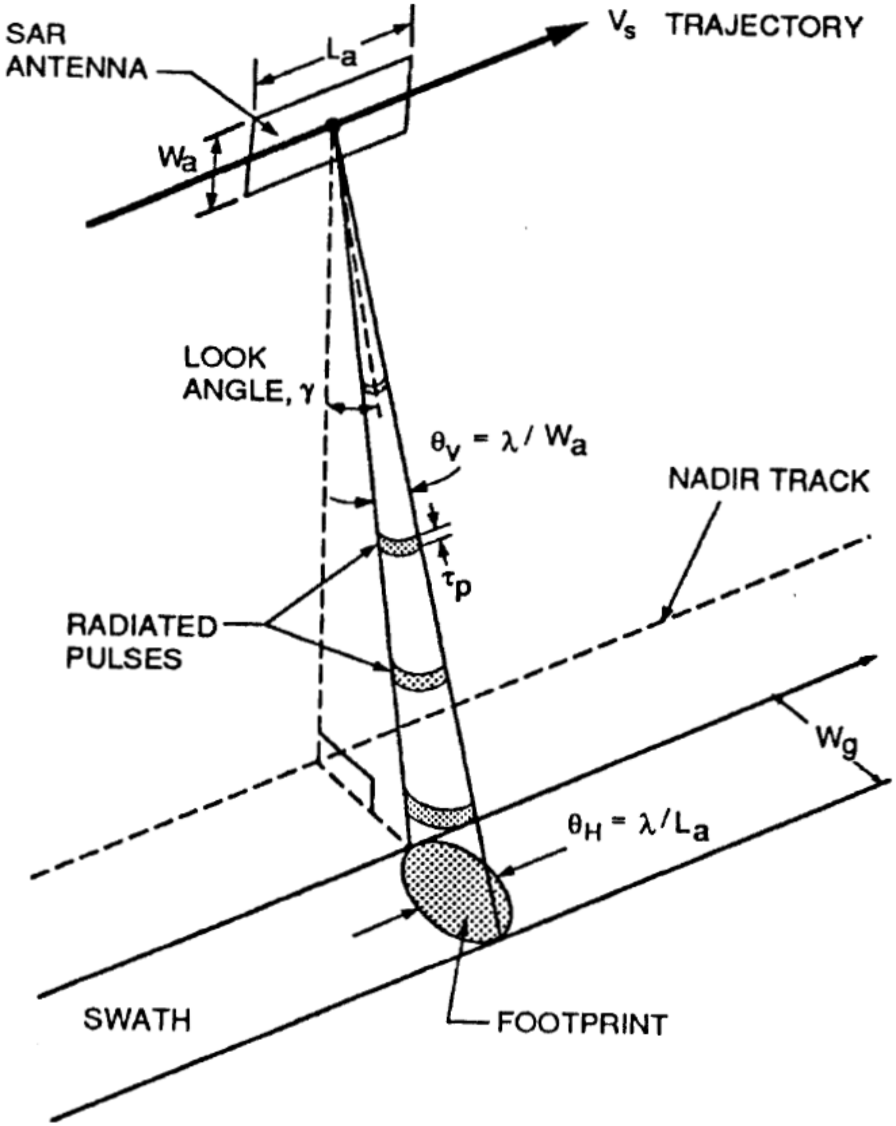

$$\theta \sim \lambda / W$$

e.g. λ = **0.05 m**

W = 10 m

θ ~ 0.005 radians

If at 800 km height, along-track footprint ~ 4 km

Trick – the Synthetic Aperture

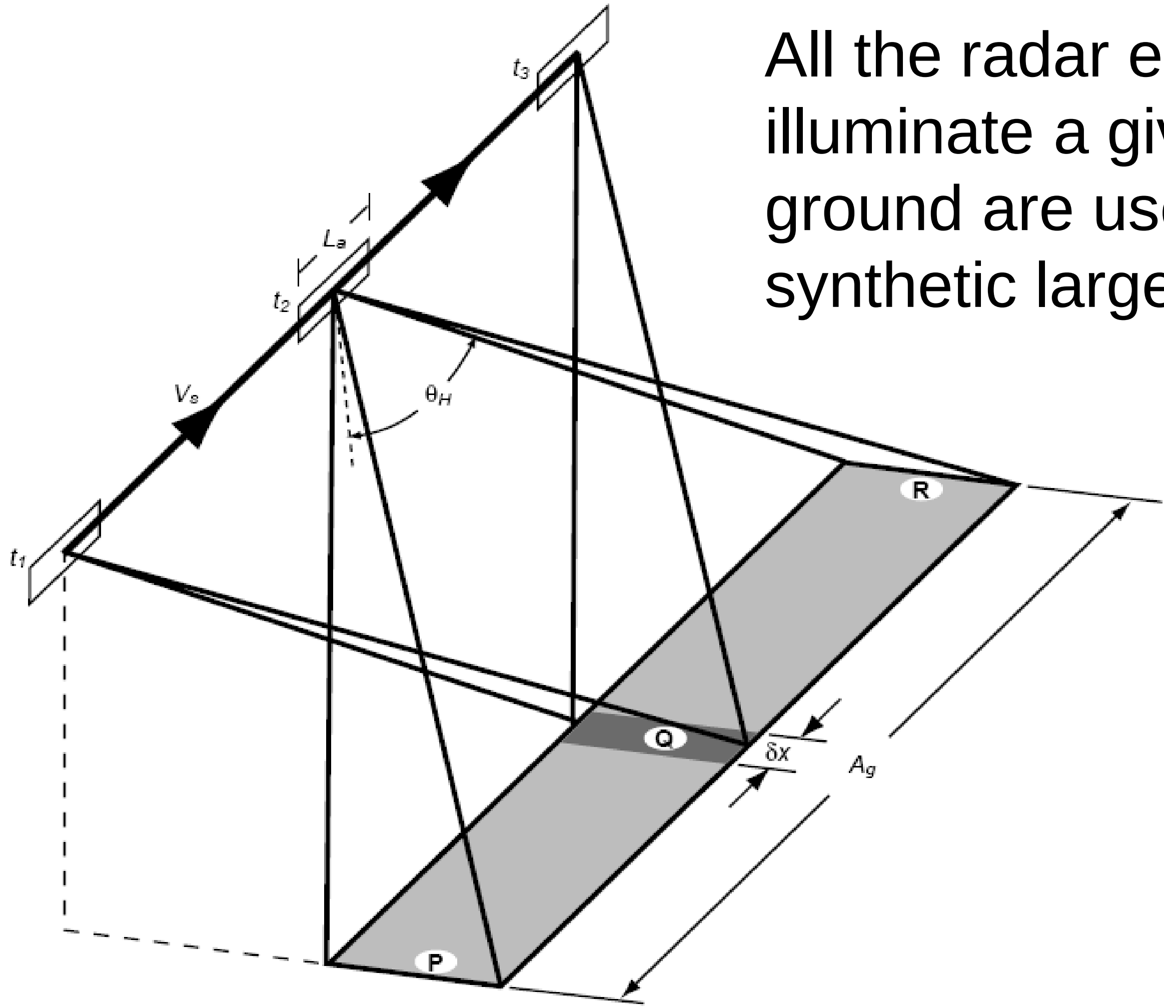

All the radar echoes that illuminate a given patch of ground are used to construct a synthetic larger antenna

Synthetic Aperture Radar (SAR)

ERS

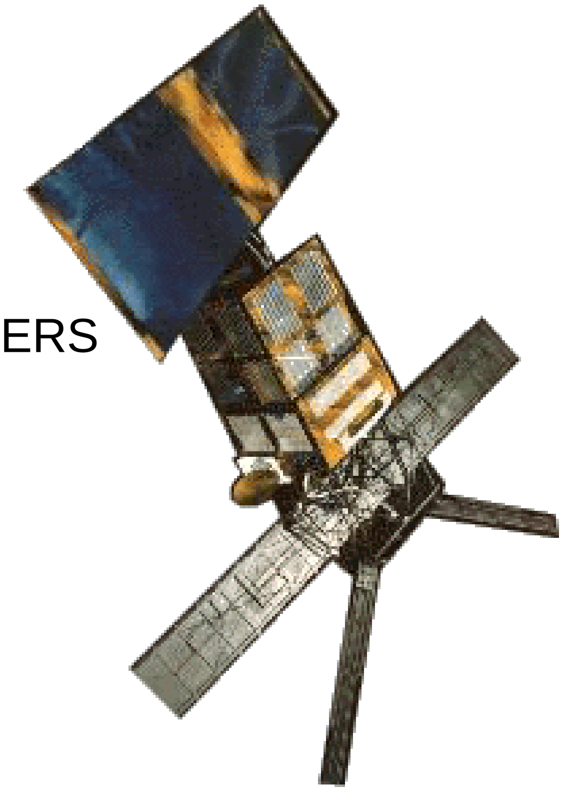

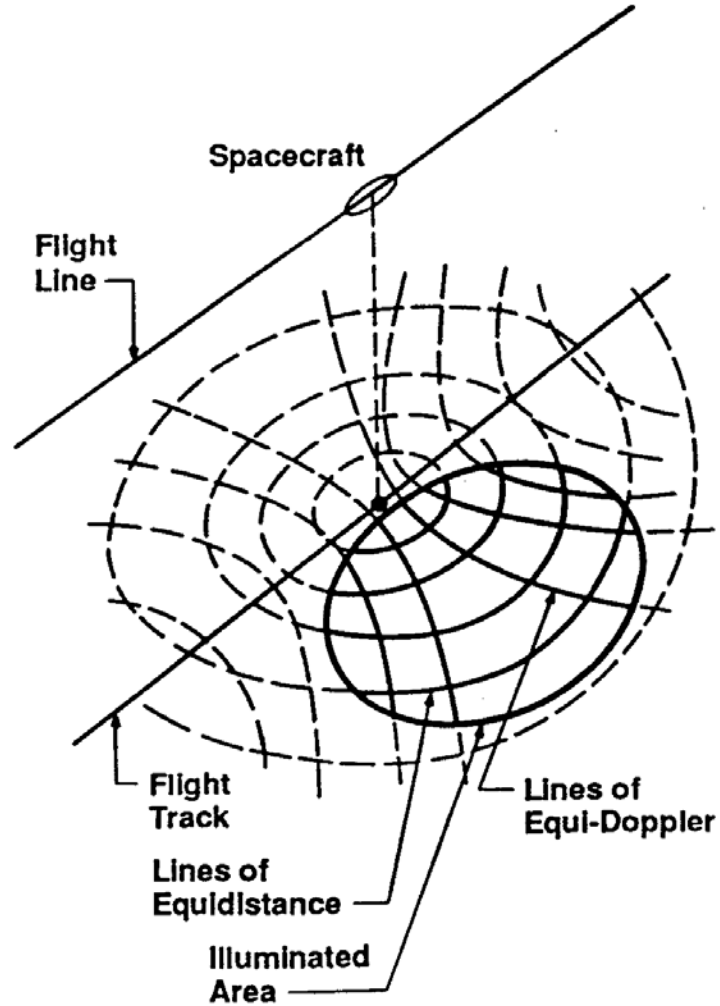

A SAR makes use of measurements of the range and Doppler shift of the radar returns to locate ground points. The signals from many returns are analysed together to image ground elements ~5x20m in size, much smaller than would be possible with a stationary antenna of the same size - hence the Synthetic Aperture.

Satellite Radar

- Active illumination
- Polar-orbiting, side-looking

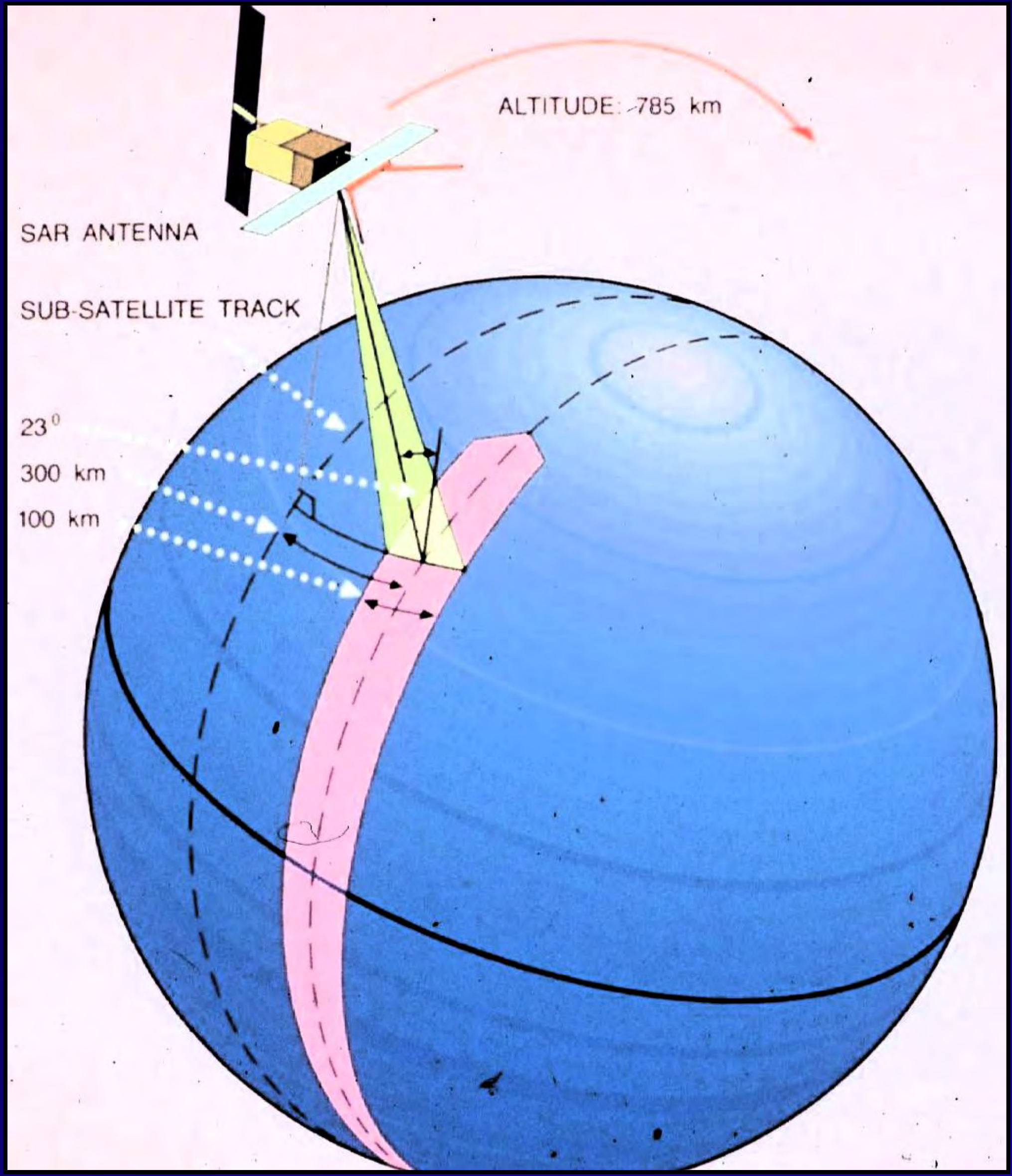

Satellite Radar

- Active illumination
- Polar-orbiting, side-looking
- European Satellites (ERS-1/2, Envisat…)
  - Stable orbits and precise pointing
  - ~10 by 2 m antenna
  - C-band (5.6cm) wavelength
  - ~20 year time series
  - Coherent illumination source
  - Sentinel-1 is the latest ESA SAR satellite, launched April 2014

InSAR – Interferometric SAR

- Phase is a function of distance from satellite to ground (range)

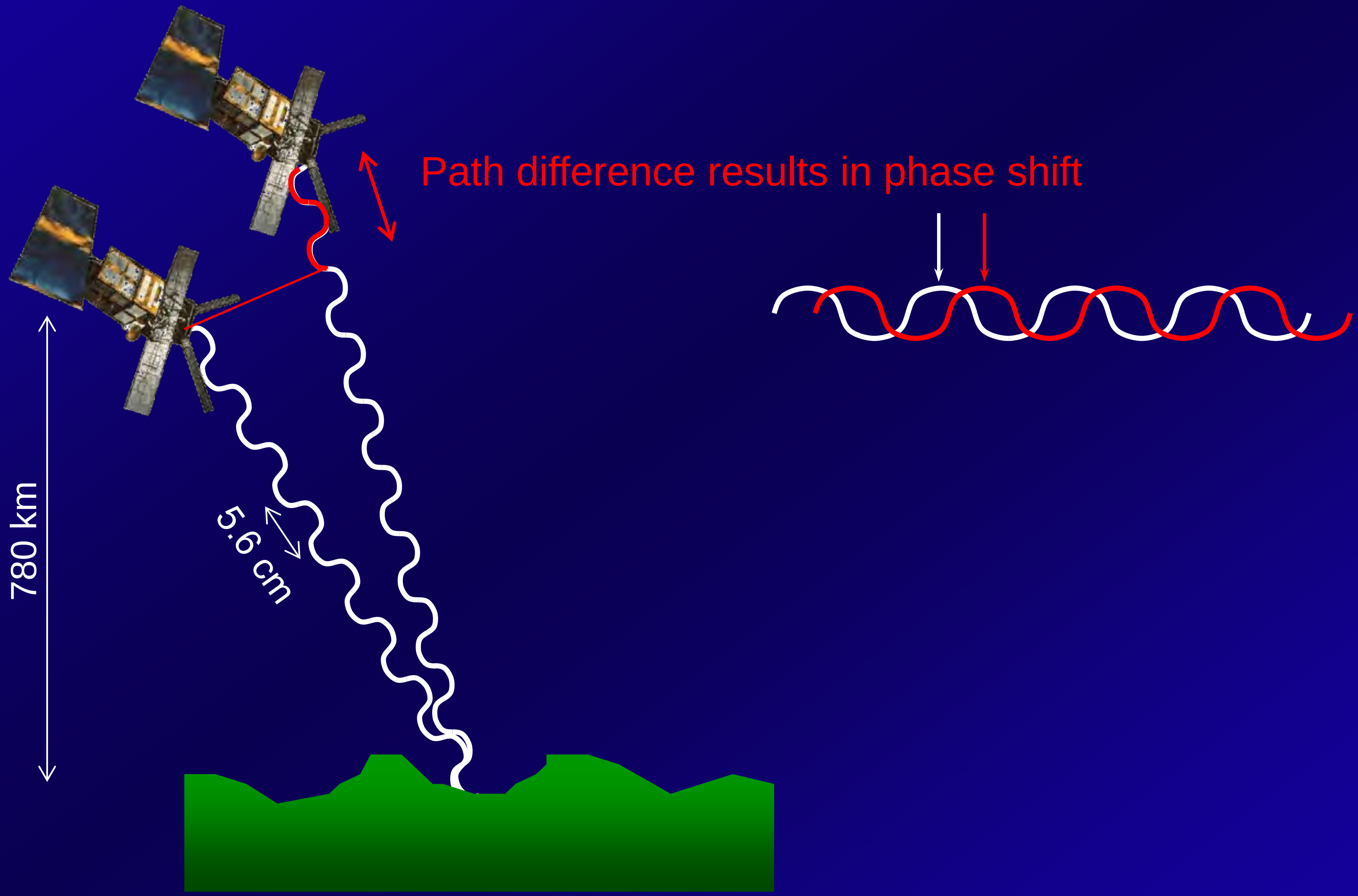

InSAR – how it works

- Phase is a function of distance from satellite to ground (range)

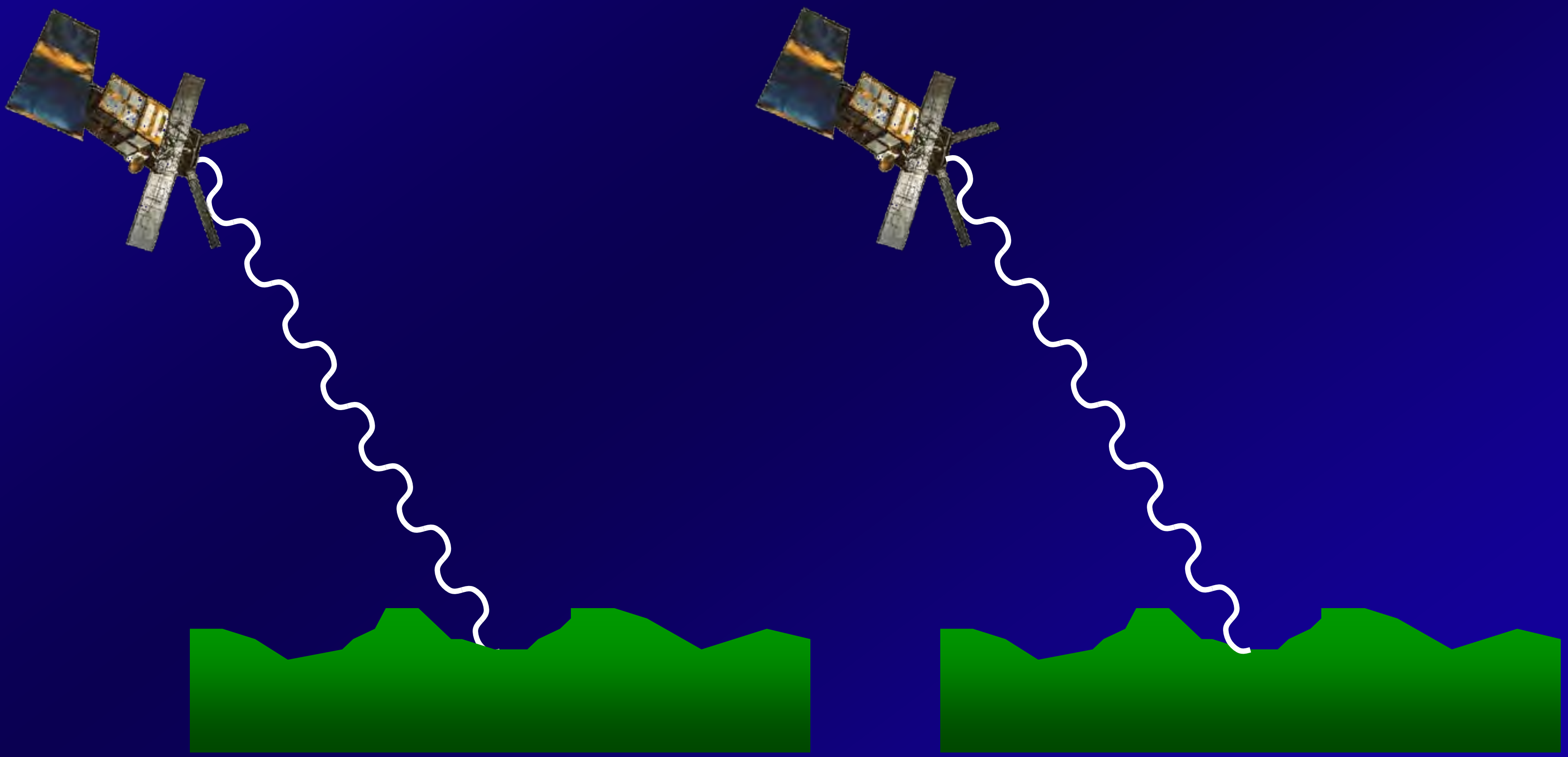

InSAR – how it works

- Phase is a function of distance from satellite to ground (range)

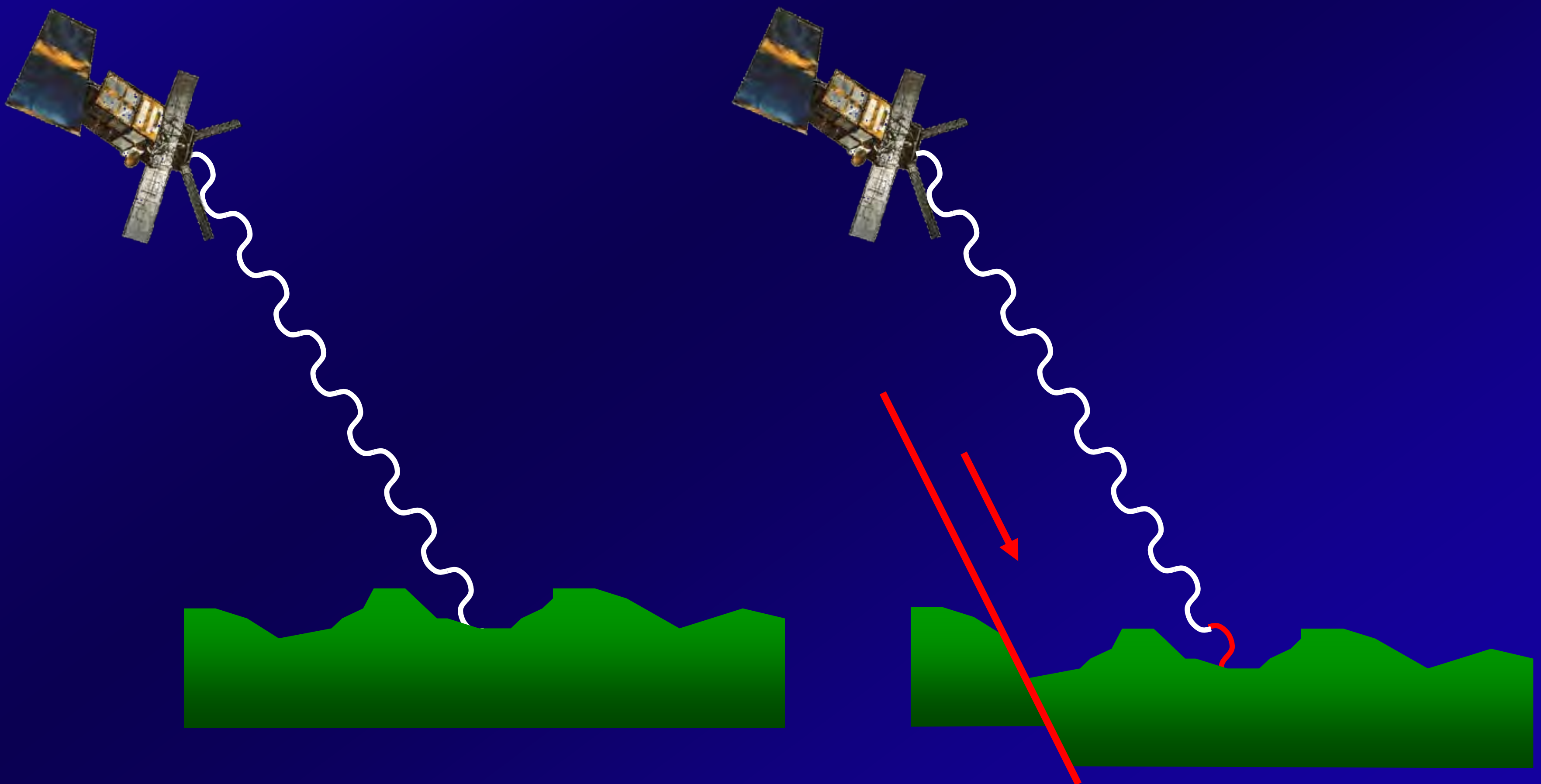

Image A - 12 August 1999

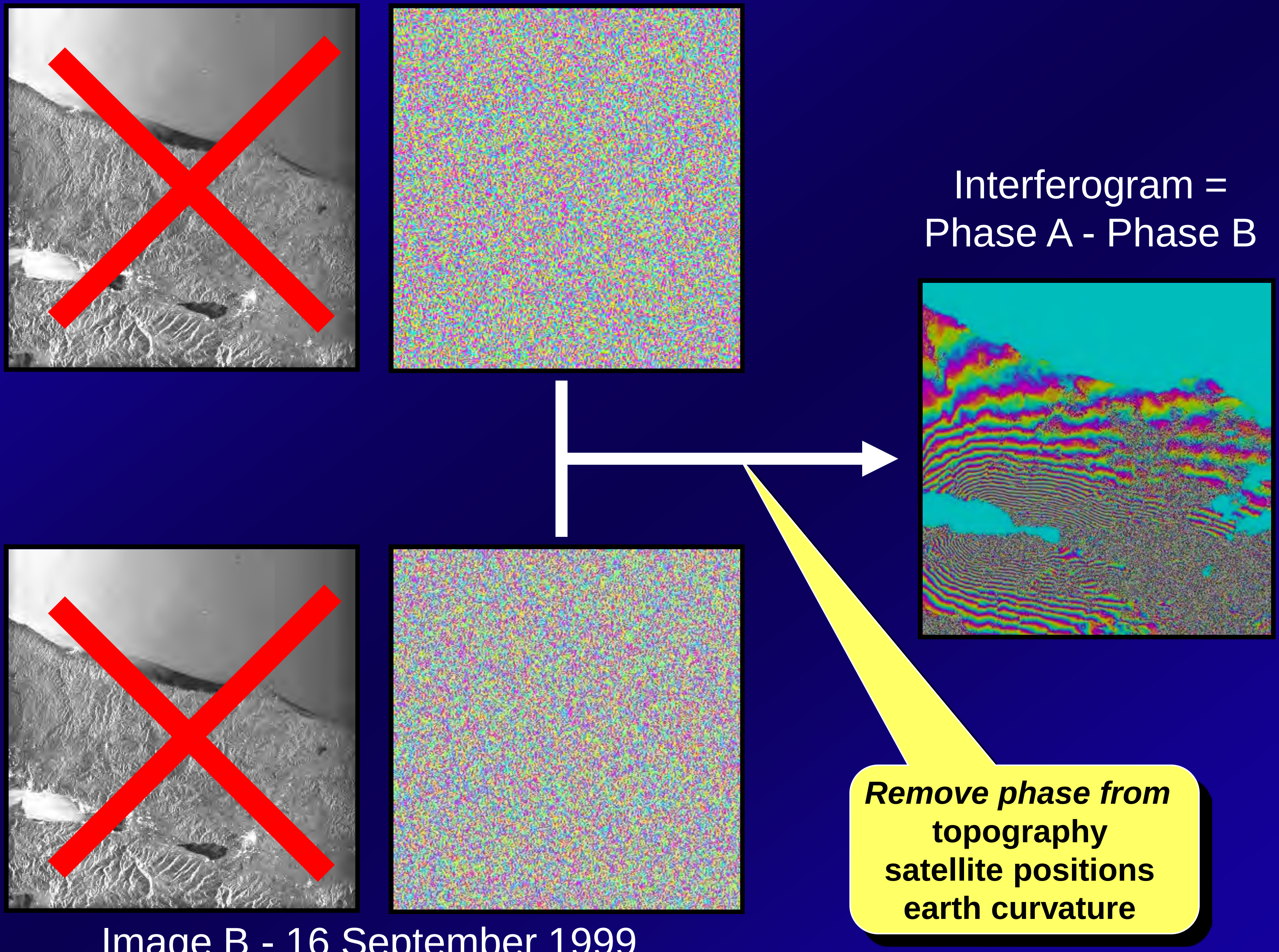

Image B - 16 September 1999

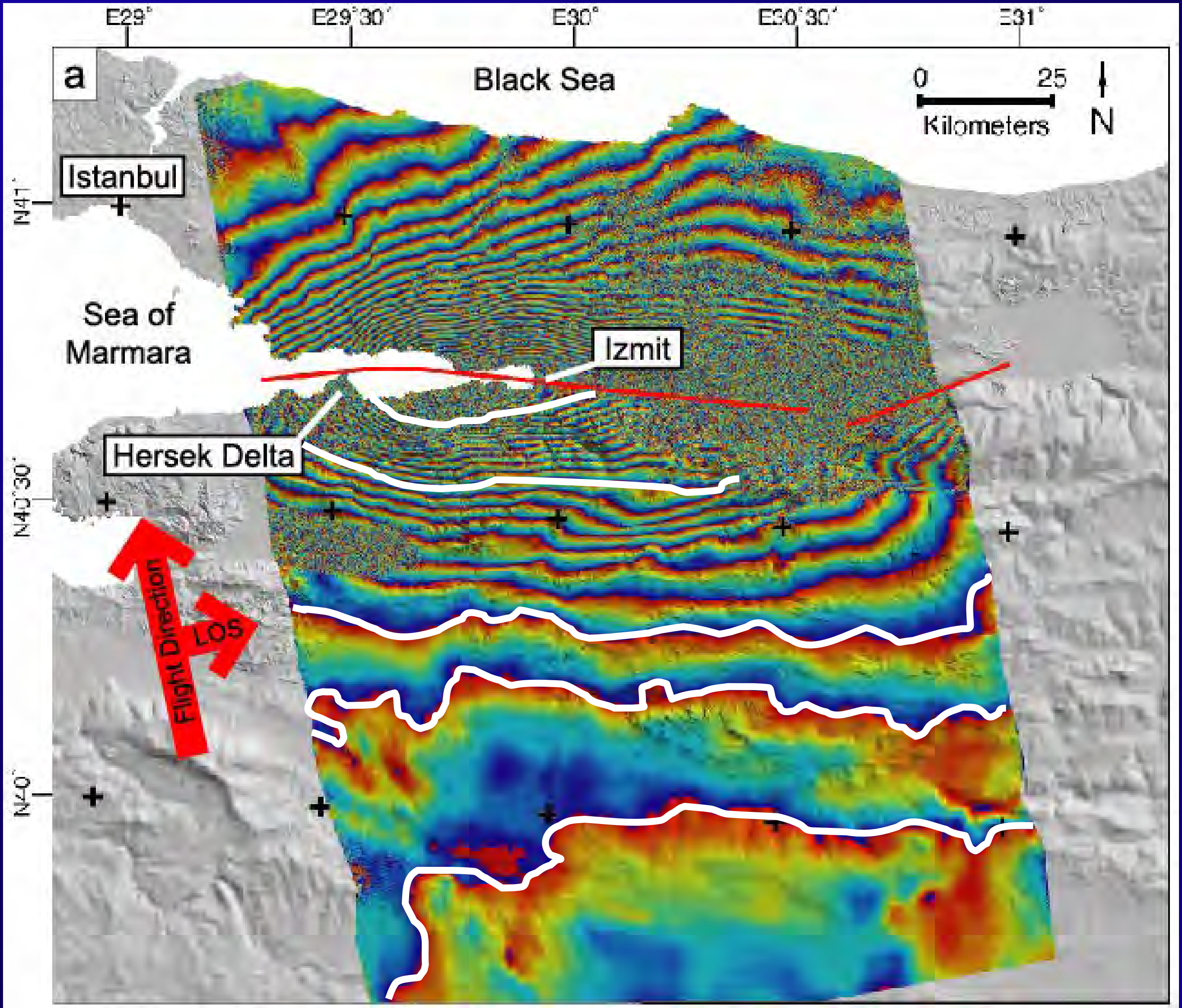

(-20) 567 mm range decrease

(-10) 283 mm range decrease

(-2) 57 mm range decrease

(-1) 28 mm range decrease

(0) 0 mm range change

17 August 1999, Izmit earthquake (Turkey)

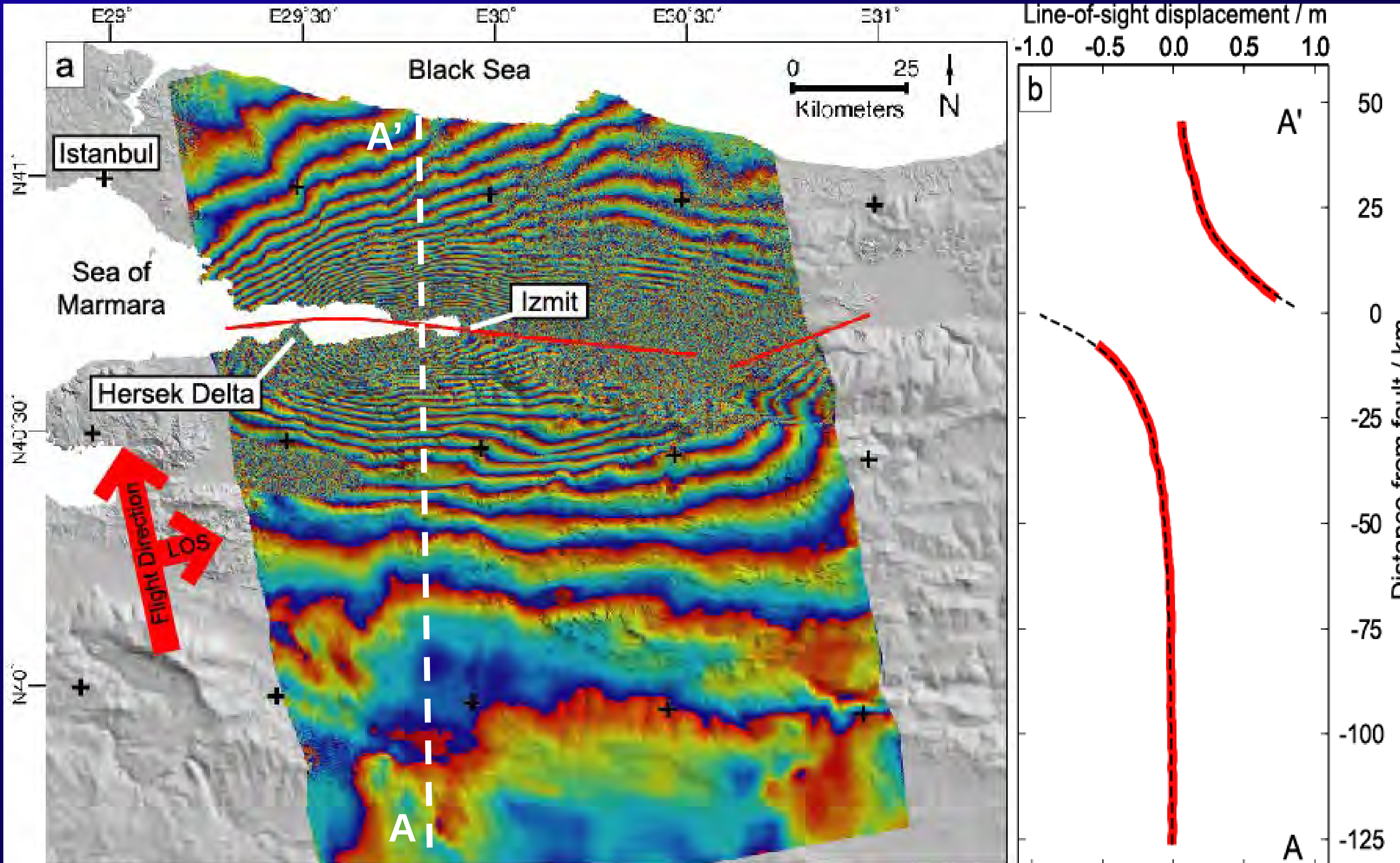

17 August 1999, Izmit earthquake (Turkey)

Components of interferometric phase

$$\Delta\phi_{int} = \Delta\phi_{geom} + \Delta\phi_{topo} + \Delta\phi_{atm} + \Delta\phi_{noise} + \Delta\phi_{def}$$

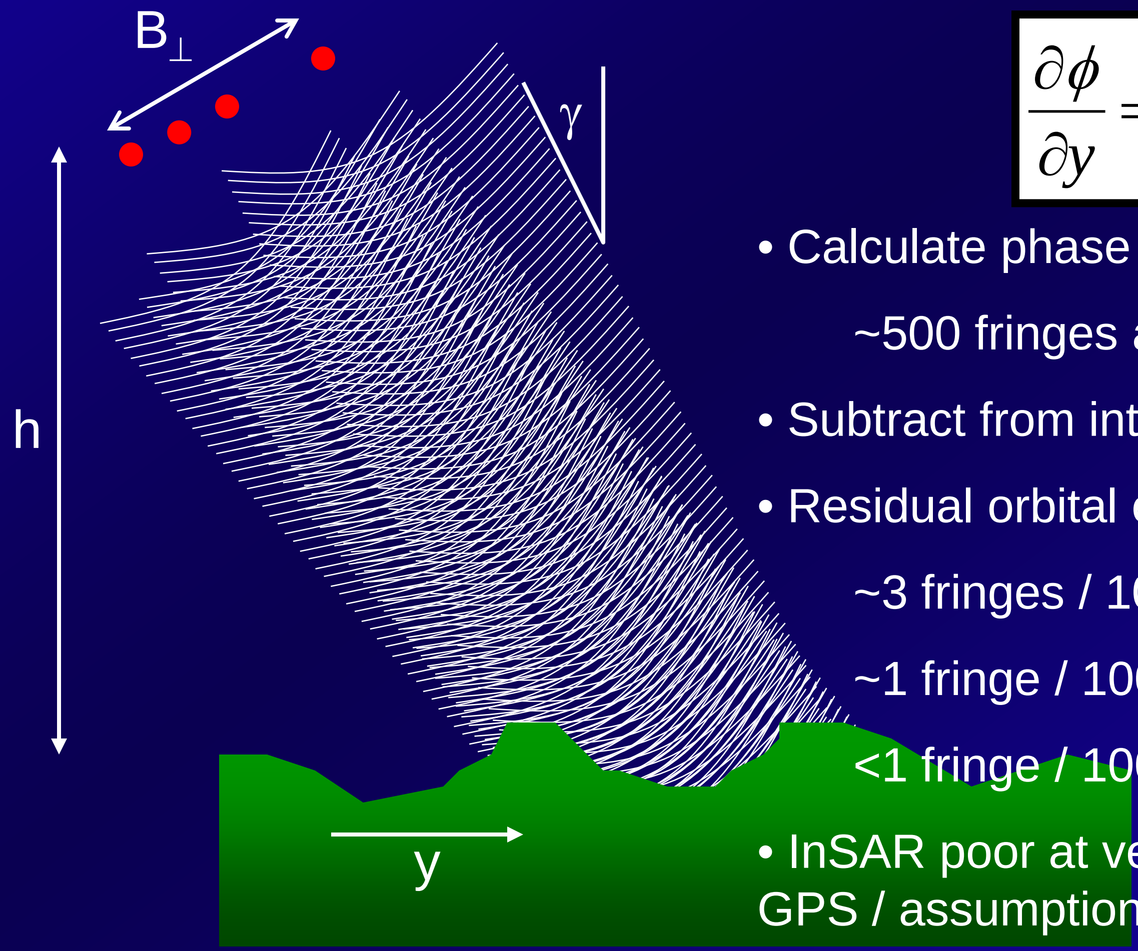

$$\frac{\partial\phi}{\partial y} = \frac{4\pi B_\perp \cos^2\gamma}{h\lambda}$$

- Calculate phase ramp from satellite orbits
  - ~500 fringes across typical frame
- Subtract from interferogram
- Residual orbital errors (for ERS):
  - ~3 fringes / 100 km across-track
  - ~1 fringe / 100 km along-track
  - <1 fringe / 100 km for Envisat, Sentinel-1
- InSAR poor at very long wavelengths (use GPS / assumptions for these).

Components of interferometric phase

$$\Delta\phi_{\text{int}} = \Delta\phi_{\text{geom}} + \Delta\phi_{\text{topo}} + \Delta\phi_{\text{atm}} + \Delta\phi_{\text{noise}} + \Delta\phi_{\text{def}}$$

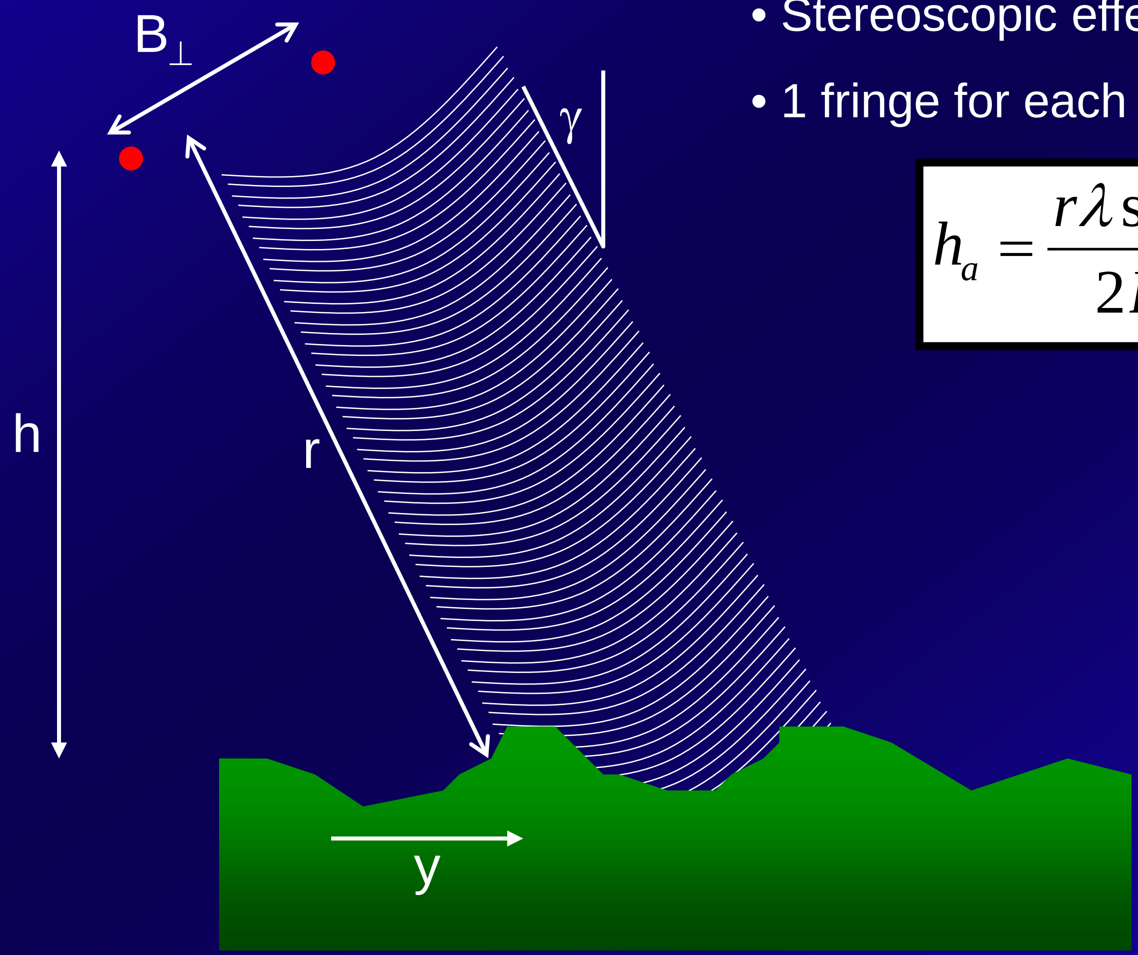

- Stereoscopic effect $\Rightarrow$ topographic fringes
- 1 fringe for each change in elevation h_a

$$h_a = \frac{r\lambda \sin\gamma}{2B_\perp} \approx \frac{10{,}000}{B_\perp}$$

(C-band, 23° incidence)

Components of interferometric phase

$$\Delta\phi_{int} = \Delta\phi_{geom} + \Delta\phi_{topo} + \Delta\phi_{atm} + \Delta\phi_{noise} + \Delta\phi_{def}$$

h_a = 500 m
$B_\perp$ = 20 m

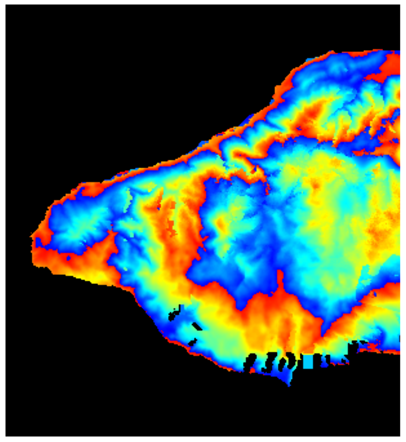

h_a = 100 m
$B_\perp$ = 100 m

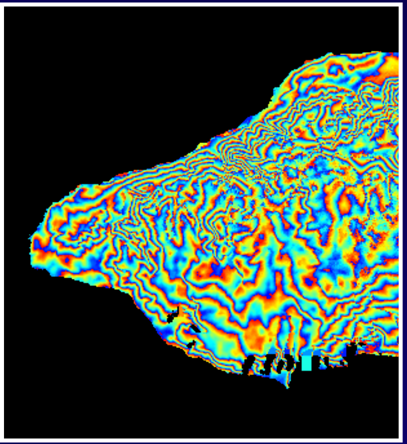

- Stereoscopic effect ⇒ topographic fringes
- 1 fringe for each change in elevation h_a

$$h_a = \frac{r\lambda \sin\gamma}{2B_\perp} \approx \frac{10{,}000}{B_\perp}$$ (C-band, 23° incidence)

- Shuttle Radar Topography Mission made use of this to map topography globally (±60°) at 30/90 m resolution.
- Using SRTM (accuracy <7m) gives topographic noise of 7/500*28 = 0.4 mm for 20 m baseline, and ~2 mm for 100 m baseline.

Components of interferometric phase

$$\Delta\phi_{int} = \Delta\phi_{geom} + \Delta\phi_{topo} + \Delta\phi_{atm} + \Delta\phi_{noise} + \Delta\phi_{def}$$

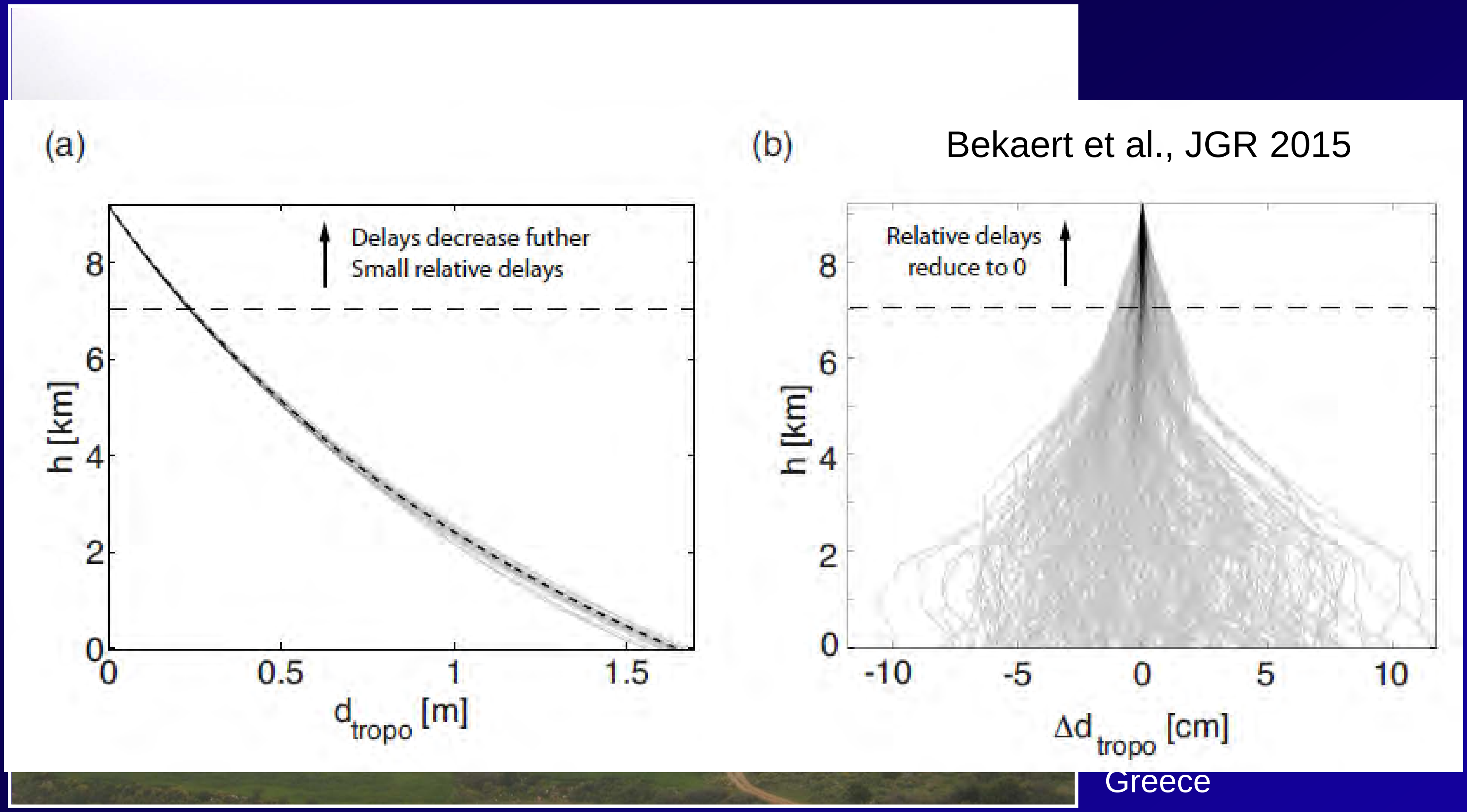

Greece

Components of interferometric phase

$$\Delta\phi_{\text{int}} = \Delta\phi_{\text{geom}} + \Delta\phi_{\text{topo}} + \Delta\phi_{\text{atm}} + \Delta\phi_{\text{noise}} + \Delta\phi_{\text{def}}$$

Layered atmosphere

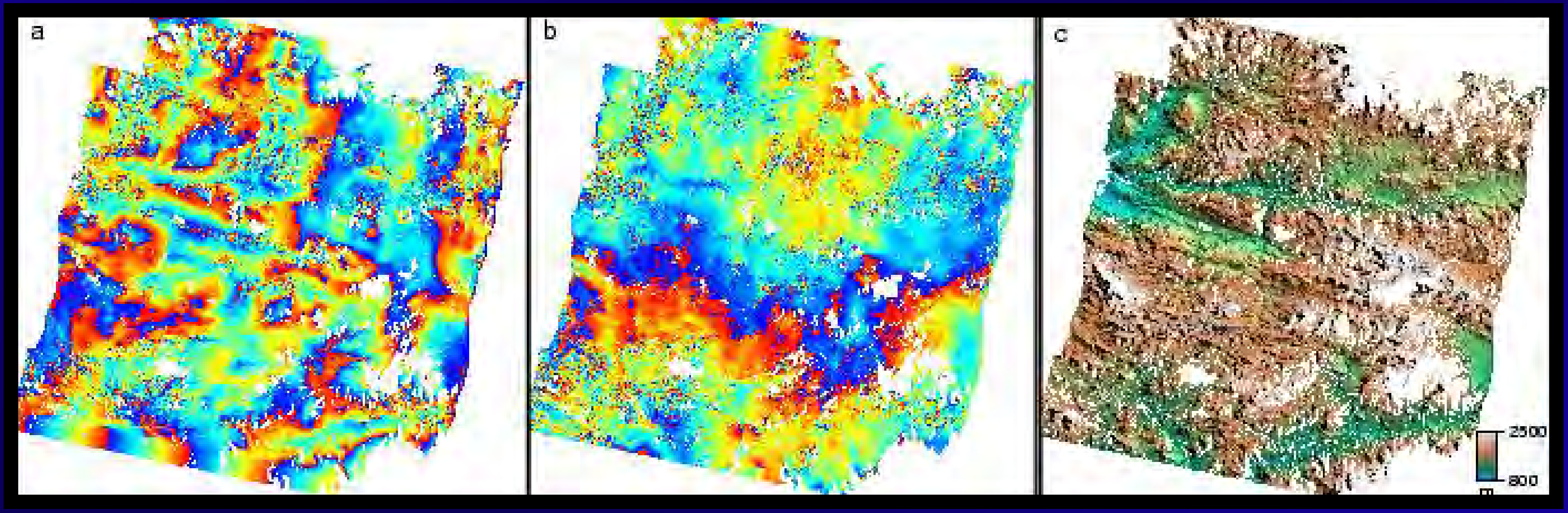

29/8/1995 to 29/7/1997 | 30/8/1995 to 29/7/1997 | Topography

Components of interferometric phase

$$\Delta\phi_{\text{int}} = \Delta\phi_{\text{geom}} + \Delta\phi_{\text{topo}} + \Delta\phi_{\text{atm}} + \Delta\phi_{\text{noise}} + \Delta\phi_{\text{def}}$$

Layered atmosphere

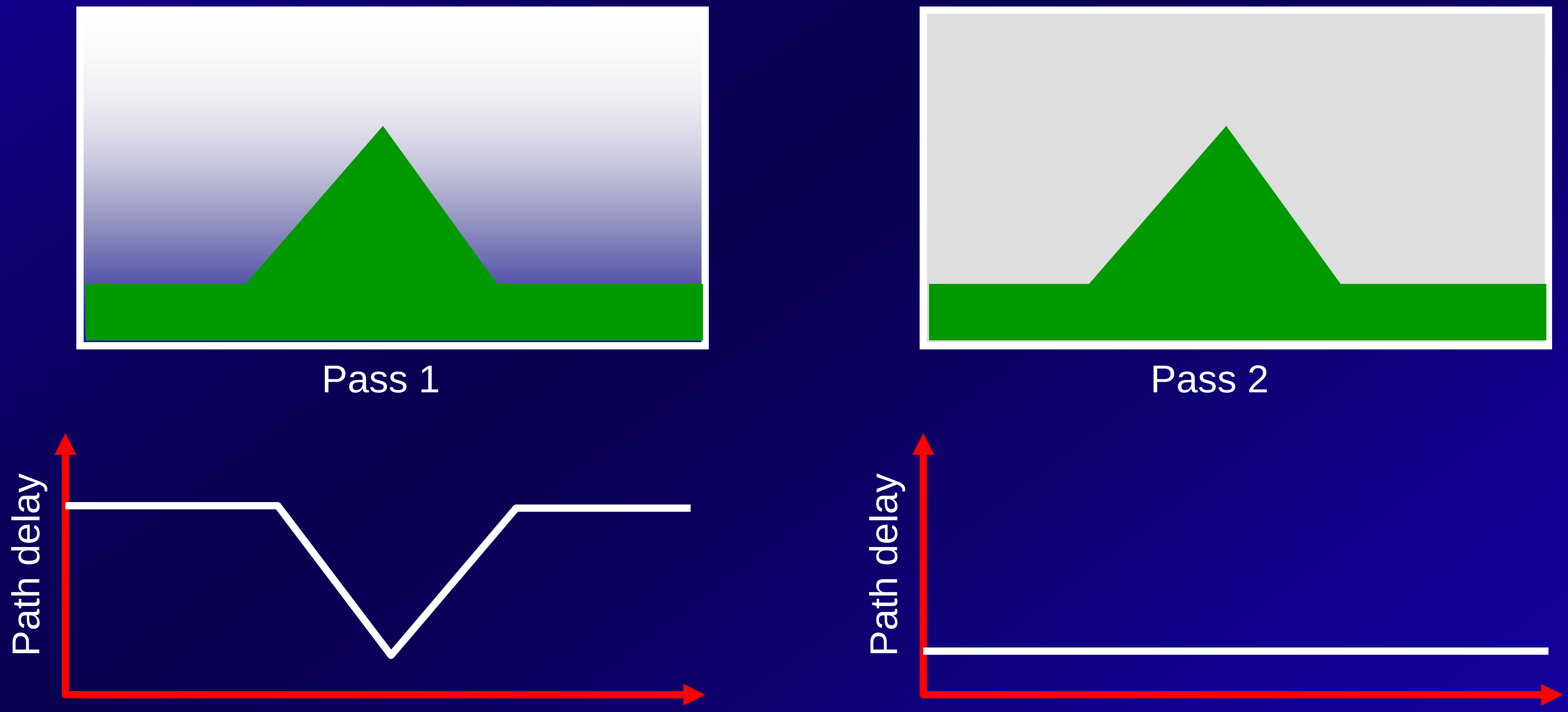

Components of interferometric phase

$$\Delta\phi_{int} = \Delta\phi_{geom} + \Delta\phi_{topo} + \Delta\phi_{atm} + \Delta\phi_{noise} + \Delta\phi_{def}$$

Turbulent atmosphere

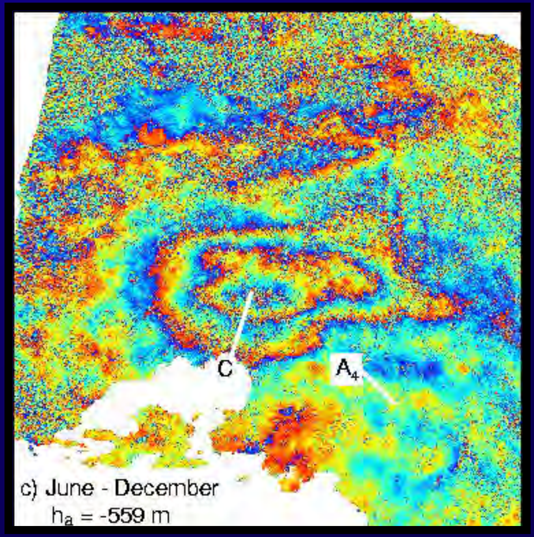

June to December

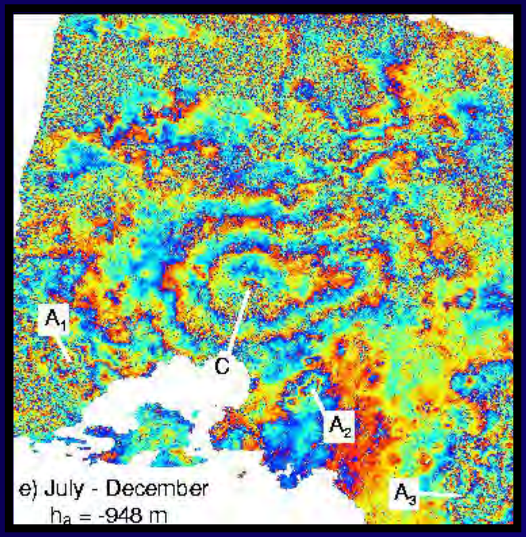

July to December

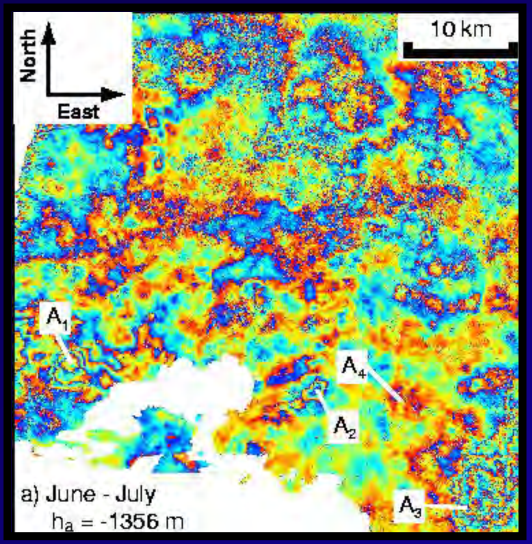

June to July

Athens Earthquake – September 1999

Components of interferometric phase

$$\Delta\phi_{\text{int}} = \Delta\phi_{\text{geom}} + \Delta\phi_{\text{topo}} + \Delta\phi_{\text{atm}} + \Delta\phi_{\text{noise}} + \Delta\phi_{\text{def}}$$

- Size of $\Delta\phi_{\text{atm}}$ (at sea level) ~ ± 3 fringes (~100 mm) in extreme cases
- Methods for dealing with $\Delta\phi_{\text{atm}}$
  - Ignore (most common)
  - Quantify
  - Model based on other observations (e.g. GPS, meteorology…)
  - Increase SNR by stacking or time series analysis
  - Model based on relationship with topography

Components of interferometric phase

Sun et al., 2009

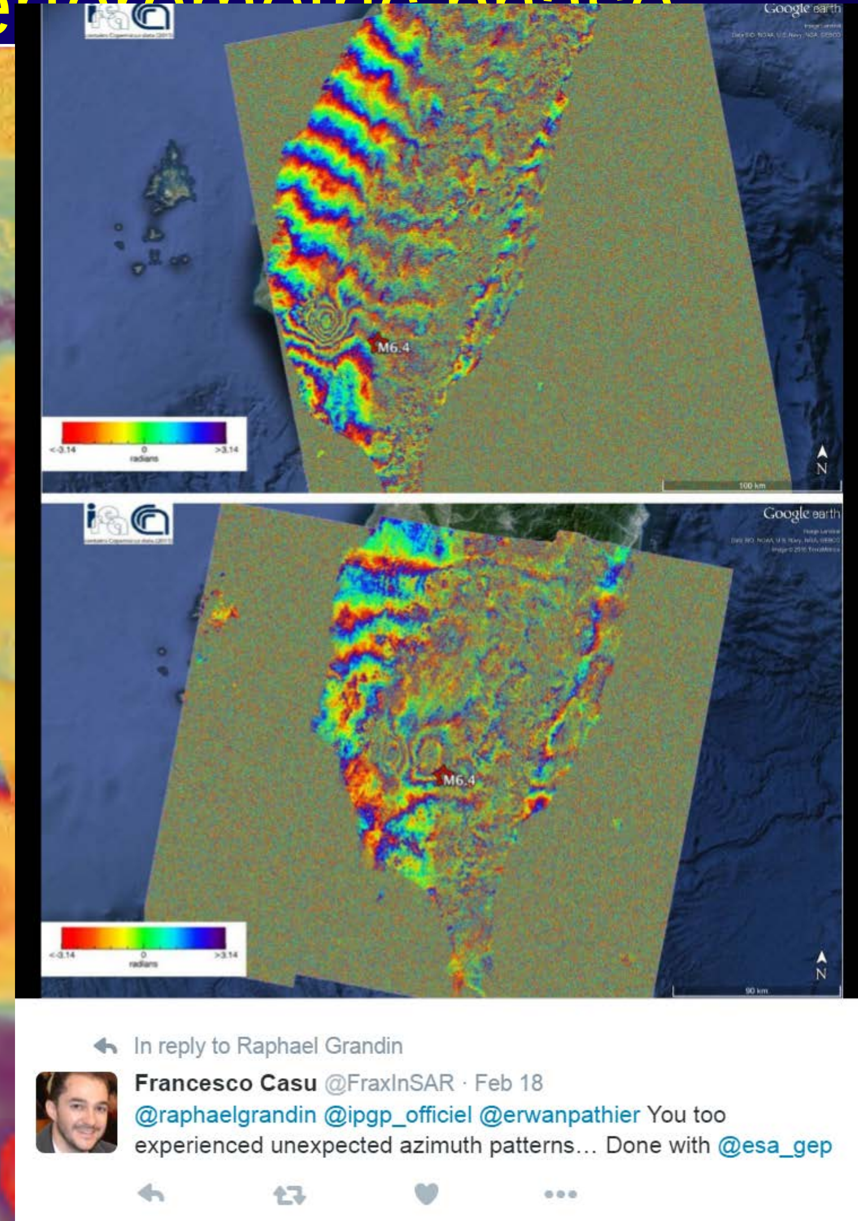

Components of interferometric phase

$$\Delta\phi_{\text{int}} = \Delta\phi_{\text{geom}} + \Delta\phi_{\text{topo}} + \Delta\phi_{\text{atm}} + \Delta\phi_{\text{noise}} + \Delta\phi_{\text{def}}$$

- Biggest source of noise is due to changing ground surface
- *Coherence* is convenient measure

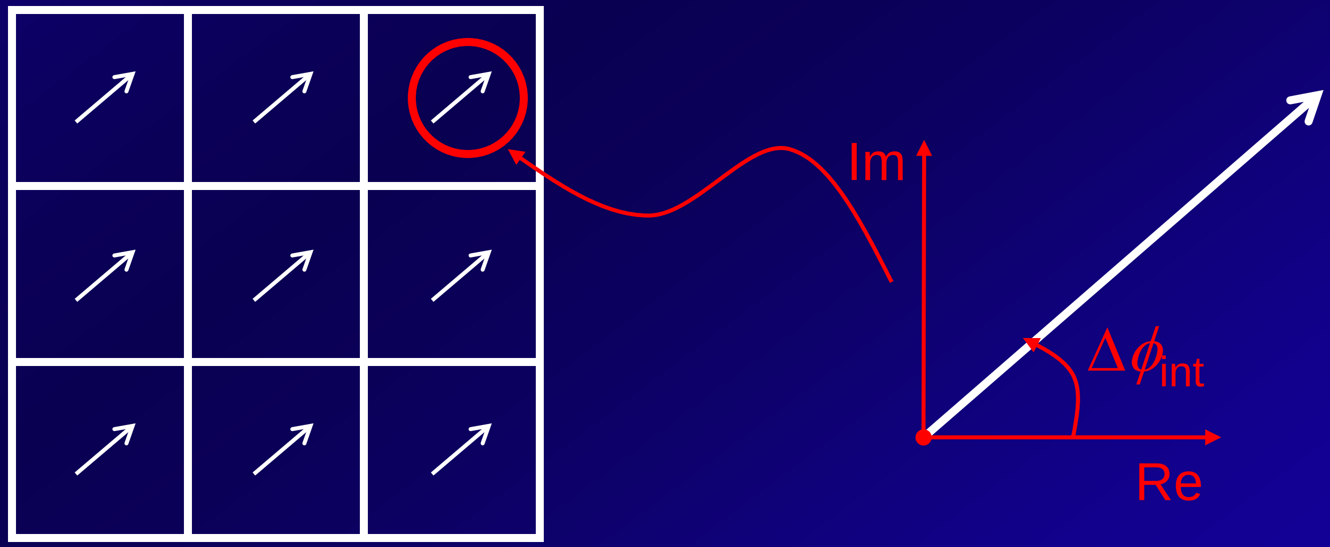

Components of interferometric phase

$$\Delta\phi_{int} = \Delta\phi_{geom} + \Delta\phi_{topo} + \Delta\phi_{atm} + \Delta\phi_{noise} + \Delta\phi_{def}$$

- Biggest source of noise is due to changing ground surface
- *Coherence* is convenient measure

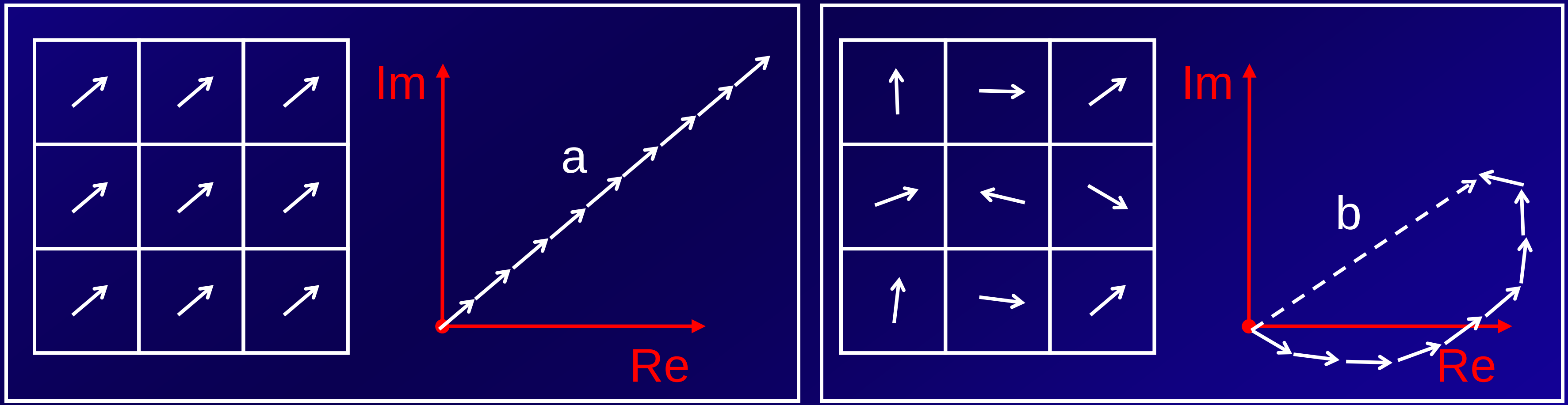

Coherence = b / a

Coherence is a function of the surface type, the time span of the interferogram, the time of year, the perpendicular baseline, changes on the ground, the weather…

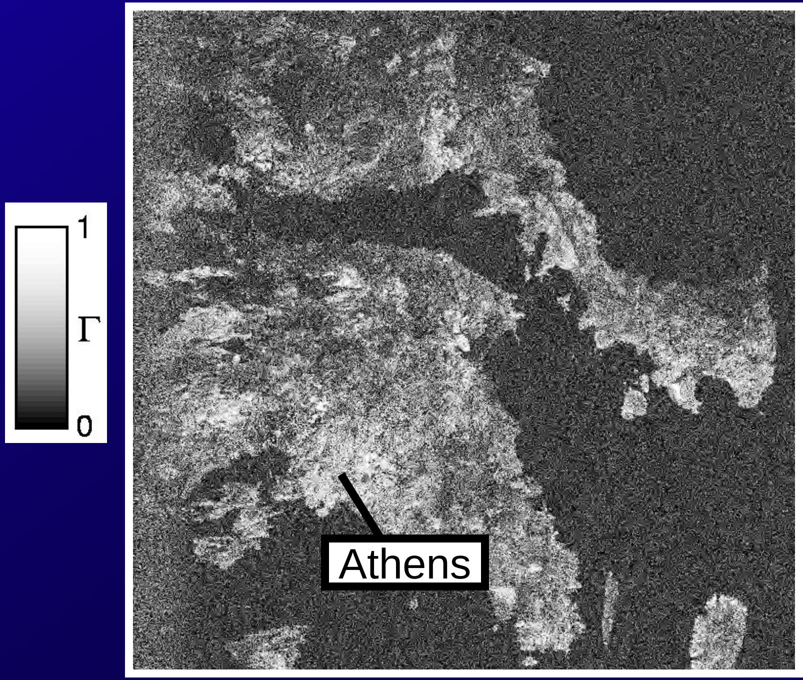

Coherent surface types

- Bare Rock
- Buildings esp. towns/cities

- Grassland
- Agricultural fields
- Ice

Incoherent surface types

- Leafy Trees
- Water

RapidSAR coherence algorithm for Ecuador Earthquake

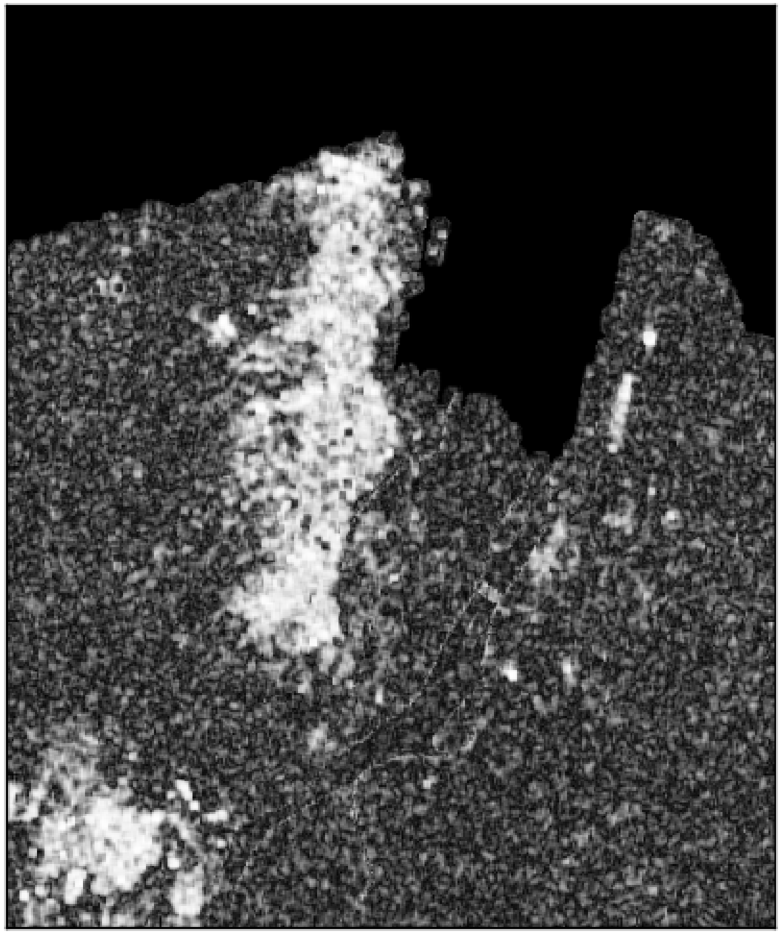

Conventional “Boxcar” Coherence

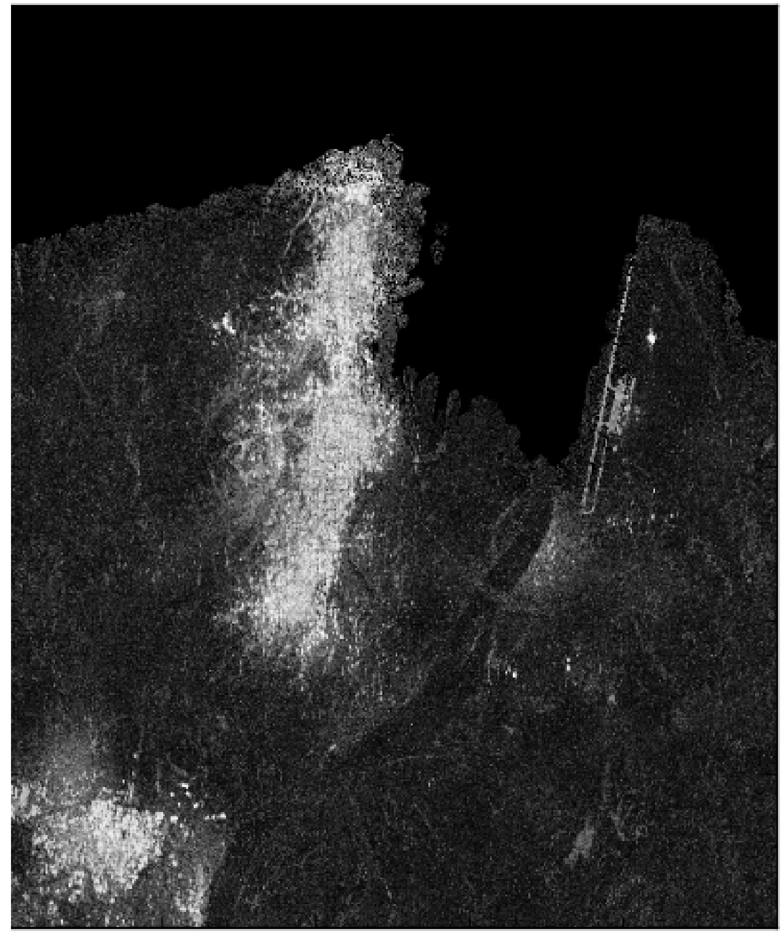

“RapidSAR” Coherence

Method: Spaans and Hooper, JGR 2016

Components of interferometric phase

$$\Delta\phi_{int} = \Delta\phi_{geom} + \Delta\phi_{topo} + \Delta\phi_{atm} + \Delta\phi_{noise} + \Delta\phi_{def}$$

1. incoherence

- Changes in the ground cover cause a random phase shift for each pixel. Best strategy is to remove pixels with low coherence.

2. Unwrapping errors

- Phase in interferograms is wrapped (each fringe is 2 π radians).
- Discontinuities or data gaps can cause phase unwrapping errors
- These can give systematic errors that are harder to deal with automatically

Components of interferometric phase

$$\Delta\phi_{int} = \Delta\phi_{geom} + \Delta\phi_{topo} + \Delta\phi_{atm} + \Delta\phi_{noise} + \Delta\phi_{def}$$

INSAR ONLY MEASURES THE COMPONENT OF SURFACE DEFORMATION IN THE SATELLITE'S LINE OF SIGHT

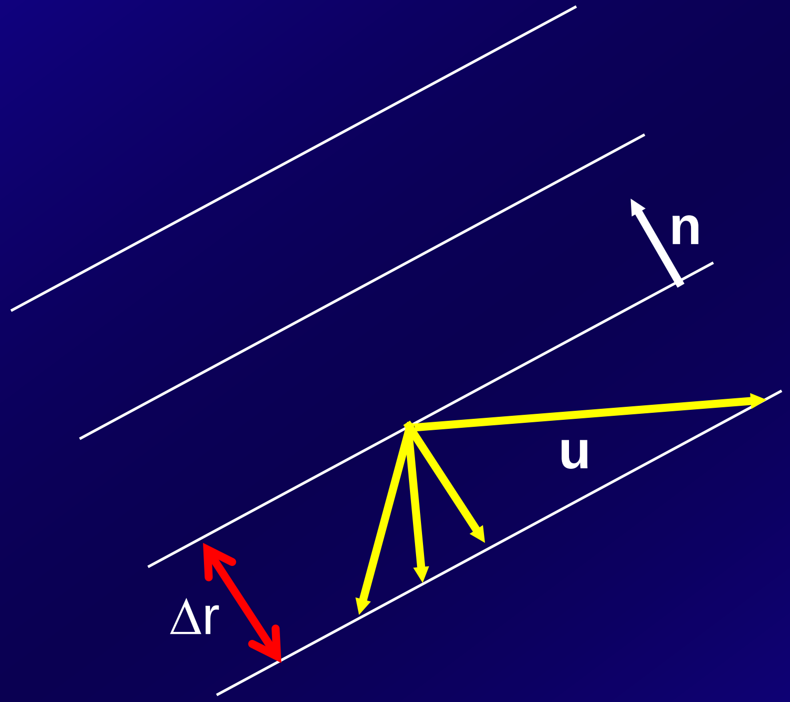

$$\Delta r = -\,\mathbf{n} . \mathbf{u}$$

where n is a unit vector pointing from the ground to the satellite

$$\Delta\phi_{def} = (4\pi / \lambda)\, \Delta r$$

i.e. 1 fringe = 28.3 mm l.o.s. deformation for ERS

Applications of InSAR

- Tectonic processes (Lecture 2)
- Volcanic Processes (Lecture 3)
- Ice motion
- Land subsidence
- Thematic mapping
- …

- 20 years of ERS, J-ERS, RSAT, ALOS, and TSX campaign-mode InSAR

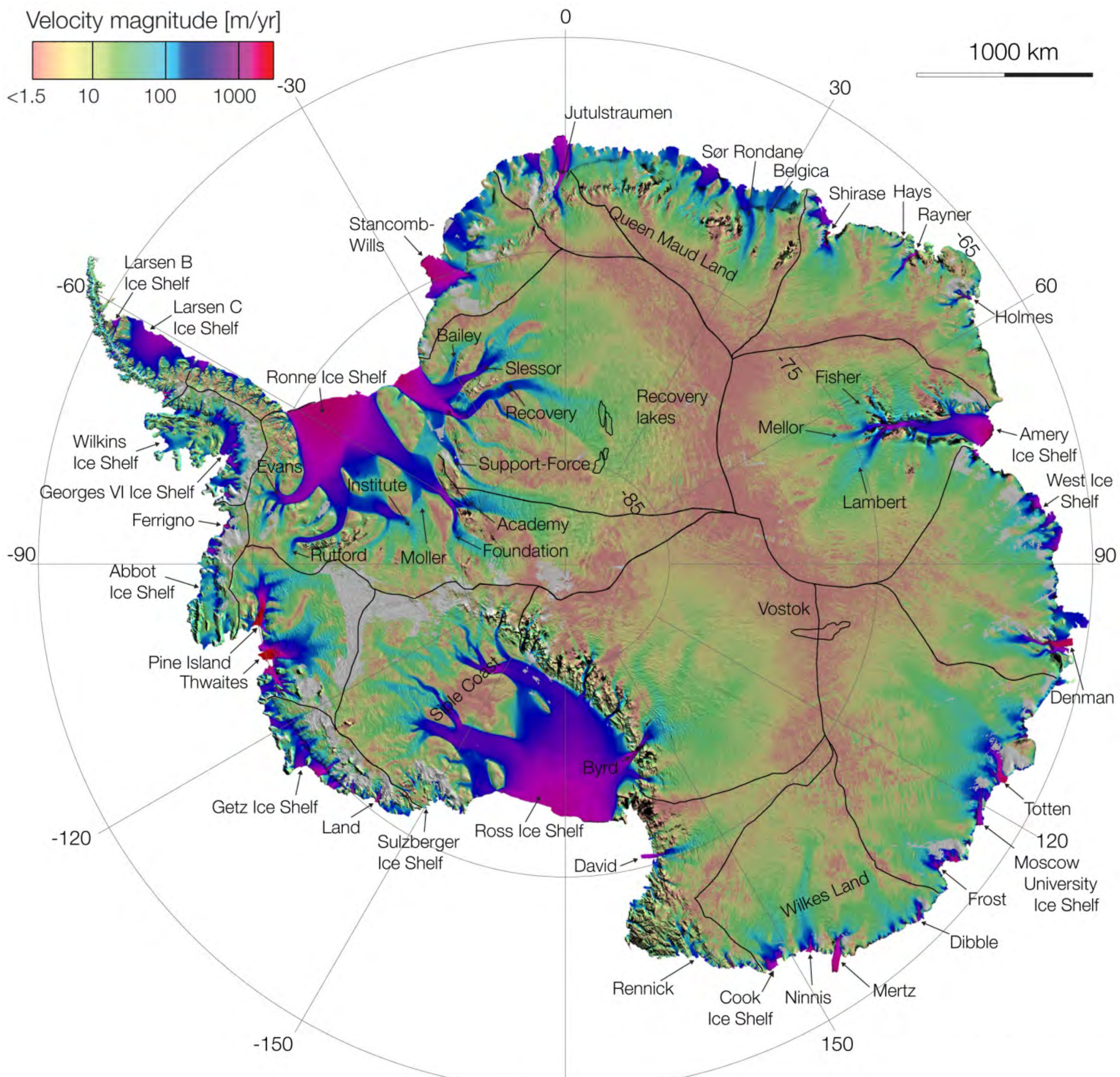

Rignot et al., 2012

Subsidence and uplift in the UK
(mostly due to long-lasting effects of coal mining)

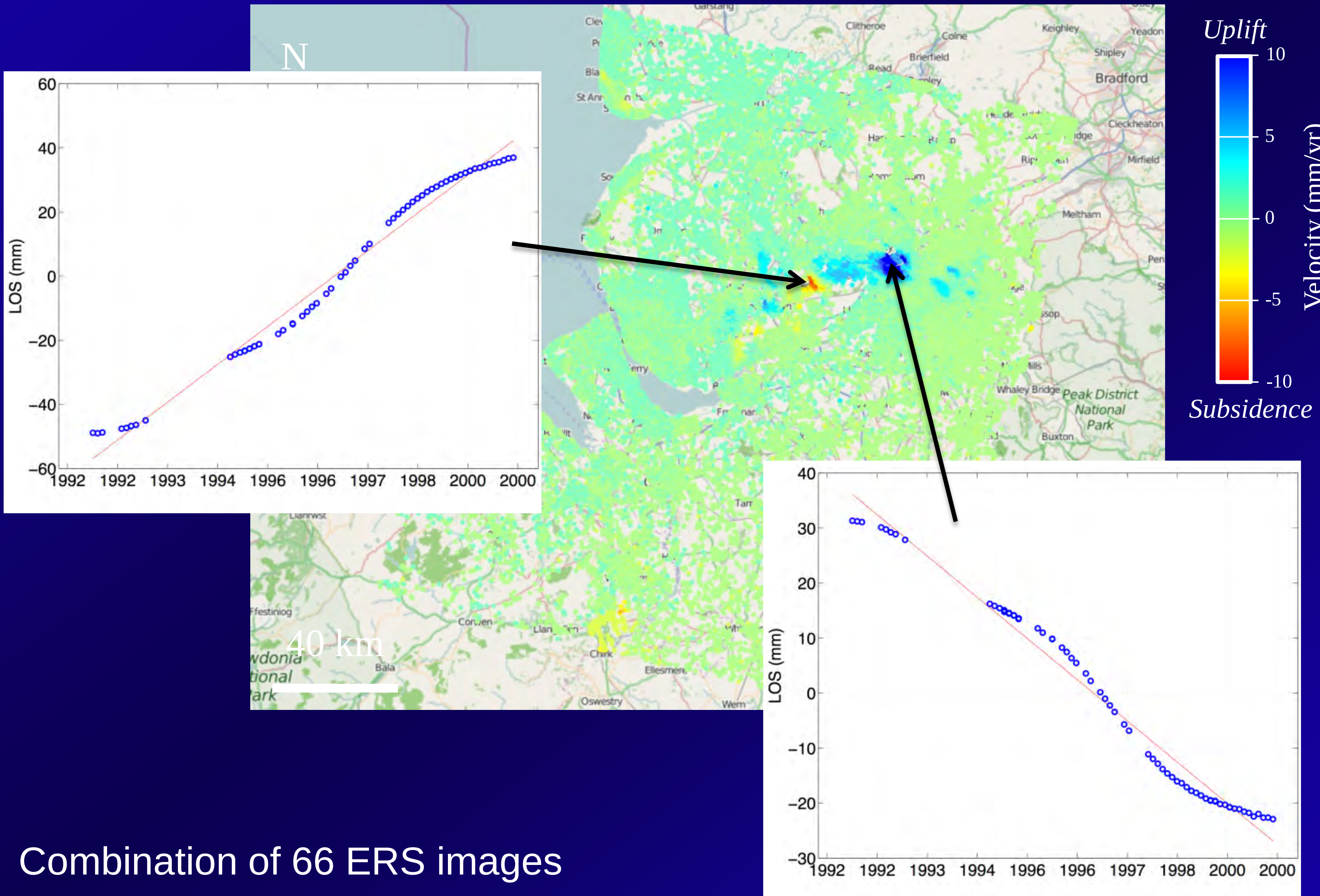

Combination of 66 ERS images

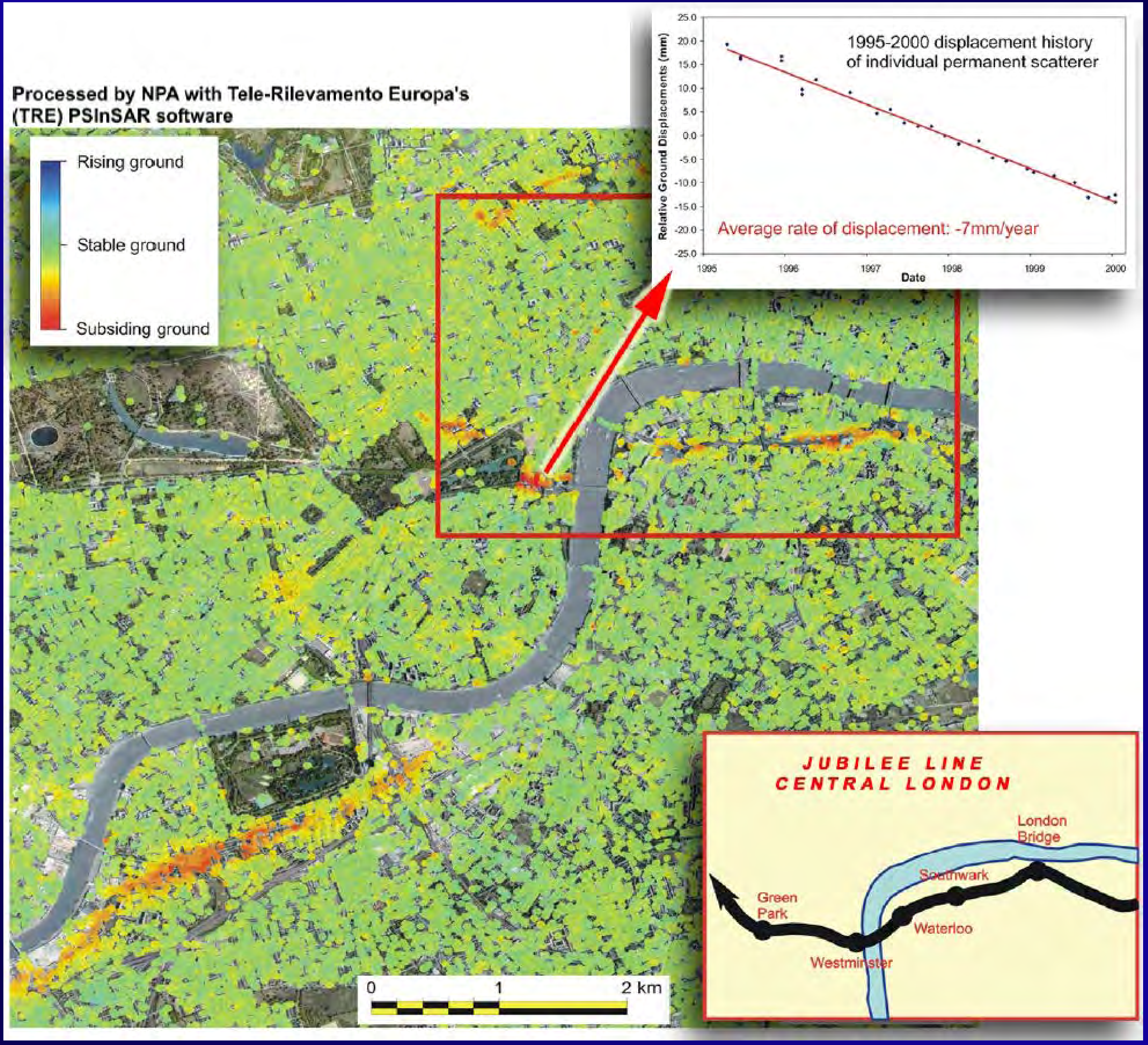
Processed by NPA with Tele-Rilevamento Europa's (TRE) PSInSAR software
Rising ground
Stable ground
Subsiding ground
1995-2000 displacement history of individual permanent scatterer
Average rate of displacement: -7mm/year
Relative Ground Displacements (mm)
Date
1995
1996
1997
1998
1999
2000
0
1
2 km
JUBILEE LINE
CENTRAL LONDON
London Bridge
Southwark
Green Park
Waterloo
Westminster

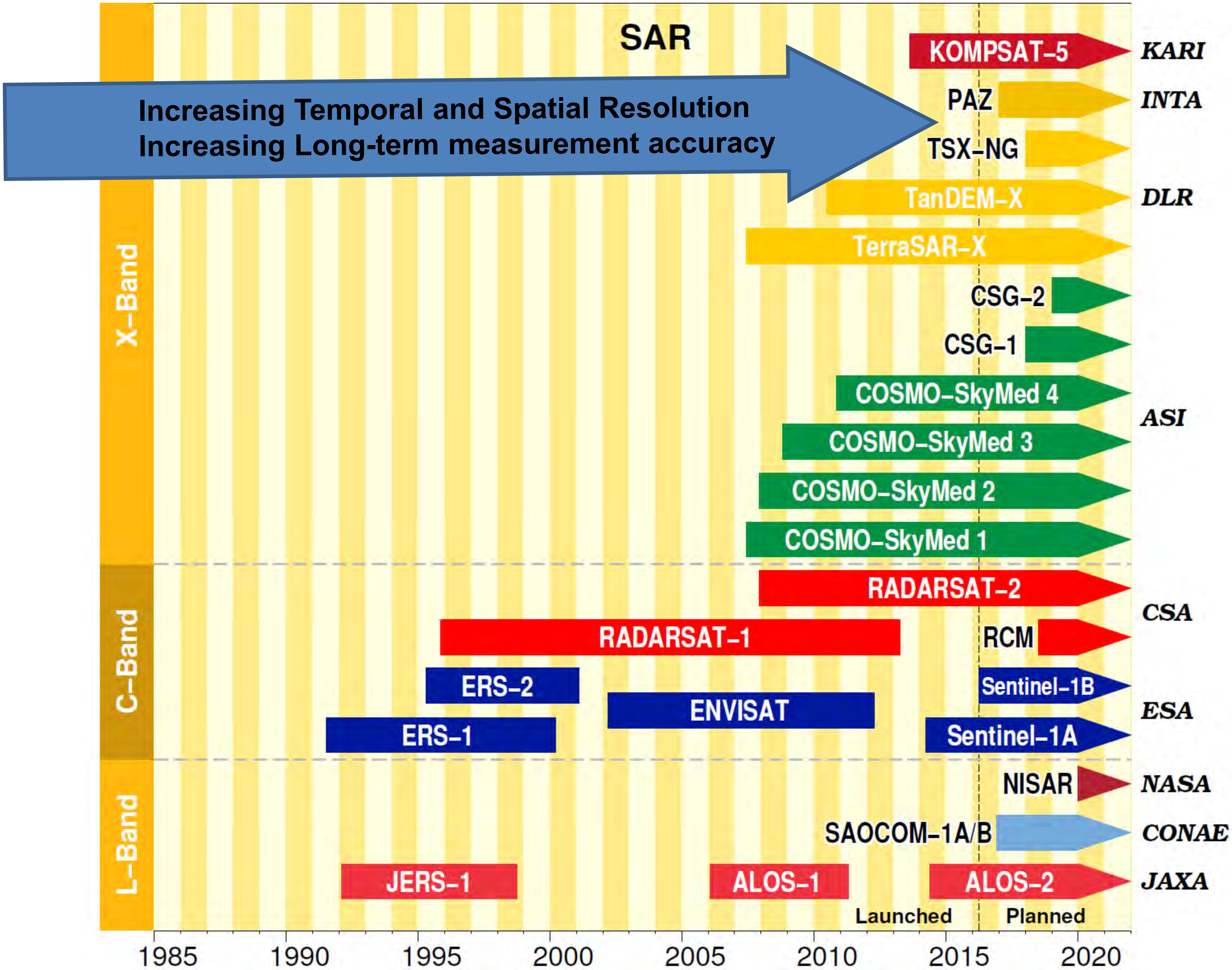
SAR
Increasing Temporal and Spatial Resolution
Increasing Long-term measurement accuracy
X-Band
C-Band
L-Band
KOMPSAT-5
PAZ
TSX-NG
TanDEM-X
TerraSAR-X
CSG-2
CSG-1
COSMO-SkyMed 4
COSMO-SkyMed 3
COSMO-SkyMed 2
COSMO-SkyMed 1
RADARSAT-2
RADARSAT-1
RCM
ERS-2
ENVISAT
Sentinel-1B
ERS-1
Sentinel-1A
NISAR
SAOCOM-1A/B
JERS-1
ALOS-1
ALOS-2
KARI
INTA
DLR
ASI
CSA
ESA
NASA
CONAE
JAXA
Launched
Planned
1985
1990
1995
2000
2005
2010
2015
2020

The Future

Sentinel-1 (EU Copernicus)

- "Operational" C-band InSAR
- 12 day repeat, 2 satellites ⇨ 3 day revisit (asc+desc)
- Funded for 20 years, Launched April 2014

BBC World News, 2 September 2014